



Cite this: DOI: 10.1039/d5gc01098e

Sonochemistry and sonocatalysis: current progress, existing limitations, and future opportunities in green and sustainable chemistry†

Quang Thang Trinh, *^a Nicholas Golio, ^b Yuran Cheng, ^{a,c} Haotian Cha, ^a Kin Un Tai, ^a Lingxi Ouyang, ^{a,d} Jun Zhao, ^e Tuan Sang Tran, ^a Tuan-Khoa Nguyen, ^a Jun Zhang, ^{a,f} Hongjie An, ^{a,d} Zuojun Wei, ^c Francois Jerome, ^b Prince Nana Amaniampong *^b and Nam-Trung Nguyen *^a

Sonocatalysis is a specialised field within sonochemistry that leverages the interaction between ultrasound and solid catalysts to enhance the rate and selectivity of chemical reactions. As a non-traditional catalytic activation method, sonocatalysis can profoundly modify reaction mechanisms and unlock novel activation pathways that are not typically accessible through standard catalysis. This unique approach offers new opportunities for driving reactions under milder conditions while potentially improving selectivity and efficiency. This review highlights the recent progress of sonocatalytic applications in green chemistry and their contribution to the United Nations' Sustainable Development Goals (SDGs), including environmental remediation, sonotherapy, and biomass conversion. In these applications, we explore the underlying sonocatalytic mechanisms and the interaction between solid catalysts and ultrasound, which drive the enhanced reactivity. A key feature of this manuscript is its comprehensive analysis of the primary technical challenges in sonocatalysis, specifically its low energy efficiency and the complexity of reaction control. To address these hurdles, we examine various effective strategies, such as the incorporation of nanostructured catalytic cavitation agents and the design of advanced microfluidic sonoreactors. These innovations improve energy transfer, control bubble dynamics, and enhance catalytic activity under ultrasound. Furthermore, we implement molecular modelling to gain fundamental insights into the mechanisms fundamental to the effectiveness of sonocatalysts. This approach provides a deeper understanding of how nanostructured catalysts interact with ultrasonic fields, guiding the design of next-generation catalytic materials. The integration of nanostructured catalytic cavitation agents, microfluidic reactor technologies, and computational molecular modelling forms a trilateral synergistic platform that unlocks new potential in sonocatalysis. This multidisciplinary framework paves the way for significant advancements in green and sustainable chemistry, offering innovative solutions to global challenges in energy, health, and environmental sustainability.

Received 2nd March 2025,

Accepted 7th April 2025

DOI: 10.1039/d5gc01098e

rsc.li/greenchem

^aQueensland Micro and Nanotechnology Centre, Griffith University, 170 Kessel Road, Nathan, QLD 4111, Australia. E-mail: q.trinh@griffith.edu.au, nam-trung.nguyen@griffith.edu.au

^bCNRS, Institut de Chimie des Milieux et Matériaux de Poitiers (IC2MP), Université de Poitiers, Bat B1 (ENSI-Poitiers), 1 rue Marcel Doré, 86073 Poitiers, France.

E-mail: prince.nana.amaniampong@univ-poitiers.fr

^cKey Laboratory of Biomass Chemical Engineering of the Ministry of Education, College of Chemical and Biological Engineering, Zhejiang University, Hangzhou, Zhejiang, 310058, P.R. China

^dSchool of Environment Science, Griffith University, 170 Kessel Road, Nathan, QLD 4111, Australia

^eDepartment of Biology, Hong Kong Baptist University, Hong Kong, China

^fSchool of Engineering and Built Environment, Griffith University, 170 Kessel Road, Nathan, QLD 4111, Australia

†Electronic supplementary information (ESI) available. See DOI: <https://doi.org/10.1039/d5gc01098e>

Green foundation

1. We discussed the crucial role of sonochemistry and sonocatalysis in advancing green chemistry by enabling energy-efficient, solvent-free, and environmentally friendly chemical processes.
2. Sonochemistry utilizes highly reactive species from the cavitation events to facilitate chemical reactions and eliminate the need for harsh chemicals or extreme conditions. The combination of sonochemistry and a catalyst, called “sonocatalysis”, leverages its contribution to green chemistry and allows to access chemicals that are not reachable by conventional routes. Its ability to intensify reactions while reducing energy consumption and waste generation makes it a powerful tool for sustainable and eco-friendly chemical manufacturing.
3. Despite their great potential, there exists several decisive technical hurdles of sonochemistry and sonocatalysis. This tutorial review identifies promising strategies to overcoming these problems which could allow unlocking the full potential of sonocatalysis for green and sustainably chemistry.

1. Introduction

Sonochemistry is an evolving field that explores the unique effects of ultrasound on chemical systems, with profound implications for industrial, environmental, and biomedical applications.^{1–6} Sonochemistry plays a crucial role in advancing green chemistry by enabling energy-efficient, solvent-free, and environmentally friendly chemical processes. The use of ultrasonic cavitation generates localized hotspots of high temperature and pressure, producing highly reactive species and radicals. These species drive oxidation, degradation, and synthesis reactions, eliminating the need for harsh chemicals or extreme conditions. Additionally, sonochemistry supports green synthesis of nanomaterials, promoting catalyst development with improved efficiency and recyclability. Its ability to intensify reactions while reducing energy consumption and waste generation makes it a powerful tool for sustainable and eco-friendly chemical manufacturing.

In recent years, the ability of ultrasound to enhance various chemical processes has led to its adoption in many fields such as ultrasound-assisted extraction, crystallisation, chemical syn-

thesis, material fabrication, and non-invasive therapies.^{7–11} The operational frequency range for sonochemistry typically lies between 20 kHz to 1 MHz, enabling a wide array of chemical transformations and material processing techniques that are otherwise challenging under conventional methods. The versatility and effectiveness of ultrasound have made it an indispensable tool in industries like food processing, pharmaceuticals, material science, and environmental remediation.^{12–14} One of the most striking features of sonochemistry is its ability to accelerate reaction rates, alter reaction pathways, and modify physical properties under relatively mild conditions. Unlike conventional chemical reactions, which often rely on high temperatures and/or pressures, sonochemical processes occur *via* the non-thermal effects of ultrasound, thereby providing more energy-efficient and selective routes for chemical transformations.

The primary mechanism driving many sonochemical processes is acoustic cavitation—the formation, growth, and violent collapse of bubbles in a liquid medium under ultrasonic irradiation. The random and uncontrolled nature of cavitation, both spatially and temporally, poses significant chal-



Quang Thang Trinh

*Dr Quang Thang Trinh completed the PhD in Chemical and Biomolecular Engineering at the National University of Singapore (NUS) in 2014. During his career, he was a Research Fellow at the Nanyang Technological University, Singapore (NTU) from 2014–2021 and a Research Scientist at the Institute of High-Performance Computing (IHPC), Agency for Science, Research and Technology (A*STAR) from 2021 to 2023. Currently, Dr Trinh is a*

Research Fellow and Program Manager at the Queensland Micro and Nanotechnology Centre (QMNC), Griffith University. His research areas focus on catalyst design and process development for sustainable chemistry in methane activation, CO₂ reduction, N₂ fixation, sono-catalysis, plasma-catalysis, plastic waste recycling and biomass conversion.



Prince Nana Amaniampong

Dr Prince Nana Amaniampong received his PhD degree in Chemical Engineering from Nanyang Technological University Singapore in 2016. He is currently a Scientist at the French National Center for Scientific Research (CNRS) with habilitation. He is also an ERC Starting Grant 2023 holder (Project ConCASM), a 2024 CNRS BRONZE MEDAL Awardee and also received the Young Researcher Prize 2022 by

the French Chemical Society (Catalysis Division). His research and career interests lie in using ULTRASOUNDS (either high or low frequencies) as alternative unconventional activation tools in assisting catalytic reactions that are generally considered sluggish and challenging. His expertise covers the catalytic conversion of bio-based substrates into industrially relevant platform and commodity chemicals.

lenges in optimising sonochemical processes. Cavitation events can occur unpredictably, leading to side reactions, unintended material degradation, and inefficient energy usage. These limitations become particularly problematic in industrial applications, where process consistency and efficiency are critical. To address these challenges, researchers have explored various strategies to better control cavitation. Traditionally, exogenous gas nuclei, such as micro- and nanobubbles, are introduced to initiate cavitation. However, microbubbles have inherent limitations, such as their short circulation half-life and rapid destruction under ultrasound. More recently, alternative nucleation agents like phase-change droplets and solid cavitation agents have been proposed. Phase-change droplets provide a more stable platform for cavitation initiation, but they still suffer from size limitations and are not suitable for long-term applications.^{15,16} Solid cavitation agents, particularly those developed for biomedical applications, offer more promise than other techniques.^{17–19} These materials, often composed of metal oxides or nanostructured surfaces, provide stable nucleation sites for cavitation and are able to be engineered for use in broader industrial applications. These agents enhance cavitation by reducing the threshold acoustic energy required, allowing for more precise control over where and when cavitation occurs.



Nam-Trung Nguyen

Dr Nam-Trung Nguyen is a professor and an ARC Laureate Fellow at the Queensland Micro- and Nanotechnology Centre (QMNC), Griffith University, Australia. He received his Dip-Ing (M. Eng.), Dr Ing (Ph. D.) and Dr Ing Habil (professorial qualification) degrees from Chemnitz University of Technology, Germany. During his career, he was a faculty member at the Nanyang Technological

*University, Singapore (NTU) from 1999 to 2013 and a Director of Queensland Micro- and Nanotechnology Centre at Griffith University from 2013 to 2023. Prof Nguyen's research focuses on microfluidics, nanofluidics, micro/nano machining technologies, micro/nano-scale science, and instrumentation for biomedical applications. He has published over 500 journal papers and filed 8 patents, of which 3 were granted. Prof. Nguyen was named as one of the **top 17 Australian researchers in Chemical & Material Sciences** by the Research Special Report of The Australian in 2020, 2021 and 2022 and continuously listed in the Stanford top 2% most influential scientists globally since 2021. In 2023, he was granted an ARC Laureate Fellowship, which is the ultimate research fellowship in Australia, to propel his exciting field of research of micro- and elastofluidics.*

Sonocatalysis, an emerging sub-field of sonochemistry, was developed to leverage the efficiencies of sonochemistry by integrating a heterogeneous catalyst into the ultrasonic field. The solid catalyst interacts with the ultrasound-induced radicals and absorbs the cavitation energy, thus facilitating more controlled reactions.^{20–26} However, the physical distance separating cavitation events and the catalytic surface limits the efficiency of energy transfer. Cavitation primarily occurs in the bulk liquid, while catalytic reactions take place on the solid surface, meaning that the full potential of the combined ultrasound-catalyst system is not realised. To overcome these challenges, several approaches are being explored. The use of nanostructured catalytic cavitation agents provides one avenue for increasing the surface area available for cavitation while reducing the energy barrier for bubble formation. These nanostructures can serve as both nucleation sites for cavitation and as active catalytic surfaces, thereby bridging the gap between ultrasound energy and catalytic activity. Another promising development is the design of microfluidic sonoreactors, which offer enhanced control over cavitation events by confining the reaction space and optimising the flow of reactants. In microfluidic systems, the interaction between ultrasound and the fluid can be precisely controlled, allowing for more uniform cavitation and reducing energy losses. In addition, the integration of computational molecular modelling is becoming increasingly important for understanding the fundamental mechanisms of sonocatalysis to better guide the design of novel nanostructured materials. By simulating the interaction between ultrasound and solid catalysts, researchers could optimise the system parameters to maximise the efficiency and selectivity.

In this review, we describe the recent developments of sonochemistry and sonocatalysis for green and sustainable chemistry. We analyse in detail the existing technical hurdles for further developing these technologies and give a perspective on harnessing the nanostructured catalytic cavitation agents and the power of microfluidics in sonocatalysis. The contribution of sonochemistry and sonocatalysis to the principles of Green Chemistry is also discussed in detailed in section 5. In this review, computational molecular modelling, nanostructured catalytic cavitation agents, and microfluidic solutions are proposed to be integrated into a sonocatalytic platform for the first time. The result is a three-pronged approach that leverages different aspects of sonochemistry to accelerate advancements green and sustainable chemistry.

2. Introduction of sonochemistry

2.1. Application of sound waves in chemistry (sonochemistry)

Sonochemistry refers to the use of sound with high-frequency vibration in the ultrasonic range as the energy source for chemical processes. The frequencies of sound are expressed in units of Hertz (Hz), where 1 Hz corresponds to one cycle of sound per second. The audible range of sound (human hearing range) is from 20 Hz–20 kHz, while sound with higher

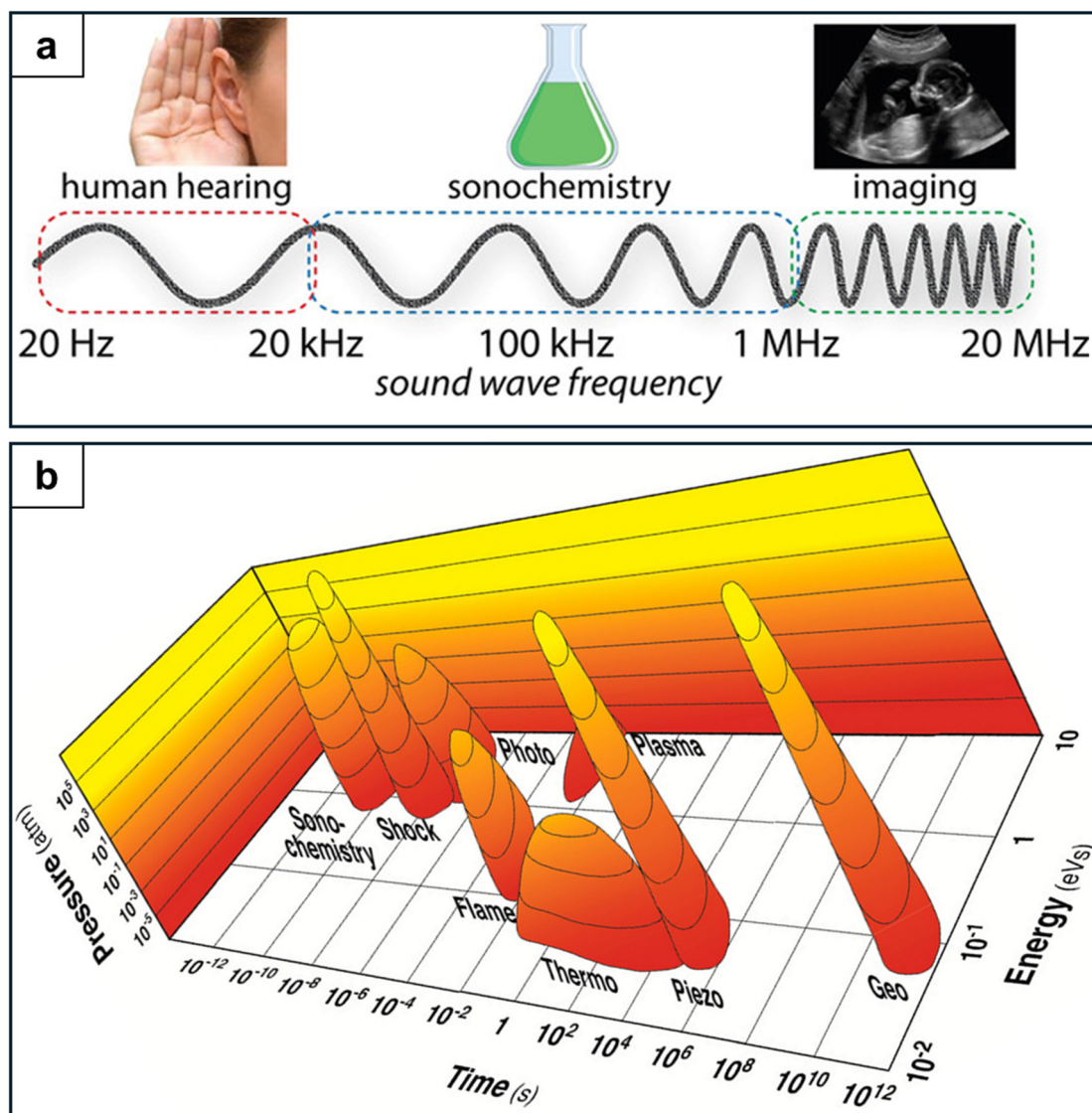


Fig. 1 (a) Frequency range of sound and their applications, reproduced with permission from McKenzie *et al.*²⁷ Copyright 2019, John Wiley and Sons. (b) Comparison of the parameters that control chemical reactivity (time, pressure, and energy) for various forms of chemistry, reproduced with permission from Suslick *et al.*²⁹ Copyright 2018, American Chemical Society.

frequencies (20 kHz–200 MHz) cannot be heard by human ears and is called “ultrasound” (Fig. 1a).²⁷ At very high frequencies, there is significant energy loss of ultrasonic irradiation due to molecular motion, resulting in negligible chemical effects. Consequently, the frequency range higher than 1 MHz is mainly used for medical imaging applications. On the other hand, the frequency range from 20 kHz to 1 MHz is of particular interest to the chemistry community since it retains enough chemical effects to carry out chemical reactions.²⁷ Under ultrasonic irradiation, cycles of bubble nucleation, growth, and collapse (referred to as cavitation) occur continuously and generate highly active radicals which are very useful in facilitating chemical reactions with high activity and selectivity.²⁸ The collapse of cavitation bubbles creates extreme local conditions of ultra-high temperature and pressure, initi-

ating free radicals which can catalyse chemical reactions. Therefore, the field of sonochemistry aims to study the effect of acoustic cavitation in liquids for enhancing chemical activity, and how cavitation affects chemical reactions and processes. The history of sonochemistry is summarised in Fig. S2 of the ESI.†

In conventional thermochemical approaches, operating parameters such as temperature, pressure, and reaction time are tuned to control the equilibrium of the chemical process. The temperature determines the amount of kinetic energy inherent in the system, and the pressure controls the interatomic collision density. Temperature, pressure, and reaction time form the three-dimensional (3D) space over which reaction conditions are tuned in order to optimise a given chemical application (Fig. 1b). However, in many cases, simply

tuning these parameters does not enable adequate control of the reaction rate and selectivity or the optimal parameters require too much energy expenditure to be a viable solution. Thus, alternative chemical pathways have emerged in an attempt to solve this bottleneck. The cornerstone of these alternative chemical pathways is that chemical reactions are driven by external triggers, such as electrical potentials (electrochemistry), photons (photochemistry), plasma (plasma-chemistry), and ultrasound (sonochemistry). Among these external triggers, ultrasound holds great promise due to its unique combination of short reaction times, high generated pressures, and high reaction energies compared to other traditional energy sources (Fig. 1b).

Fig. 1b shows that sonochemistry is characterised by the high energy amount (from 1 to 10 eV) which is introduced in a very short time ($\sim 10^{-10}$ s) and under an extremely high pressure (up to 10^3 atm). These features provide an energy equivalent comparable to shock-tube chemistry and photochemistry, except for the fact that the energy provided by ultrasound is thermal in nature. Other approaches, such as flame-chemistry in flash pyrolysis, thermochemistry, or geochemistry (the chemistry behind major geological systems), produce lower levels of energy and feature with a longer reaction duration of more than 6 orders of magnitude. Due to its unique characteristics, sonochemical reactions can occur in extreme temperature-pressure conditions in a very short duration (on the order of microseconds), resulting in unprecedented high activity and selectivity.

2.2. Acoustic cavitation: the engine of sonochemistry

Ultrasonic waves locally change the density of the fluid and are measured as pressure perturbations. With sufficient acoustic intensity, these waves disrupt the tensile forces of the liquid, forming a vapor cavity, or bubble, in the liquid.³⁰ During the propagation of ultrasound in liquid media, bubbles are expanded and compressed in response to the alternate rarefaction and compression cycles of the ultrasound. This process results in the accumulation of energy inside the bubbles as their radius changes (Fig. 2a and b).^{31–33} At a certain size, bubbles implode and release their stored energy. The formation of bubbles and their subsequent size oscillation are called “cavitation”. Cavitation events are accompanied by sudden increases in local pressure (up to several MPa) and local temperature (up to thousands of degrees Celsius).^{29,34} The extent of the effect of imploding cavitation bubbles in a liquid depends on the applied frequency. For instance, Low Frequency Ultrasound (LFUS) (20–80 kHz) generates few large cavitation bubbles (~ 170 μm at 20 kHz).³² Bubble implosion during LFUS irradiation mainly induces physical effects, such as shock waves and high speed jets.³⁵ Therefore, LFUS is often used in applications such as the erosion/deagglomeration of particles and the breaking long chain polymers.

In contrast, High Frequency Ultrasound (HFUS, >100 kHz) generates a large number of small sized cavitation bubbles (5–6 μm).³⁶ The implosion of these bubbles pyrolyses the solutes to radicals and is substantially accelerated by the

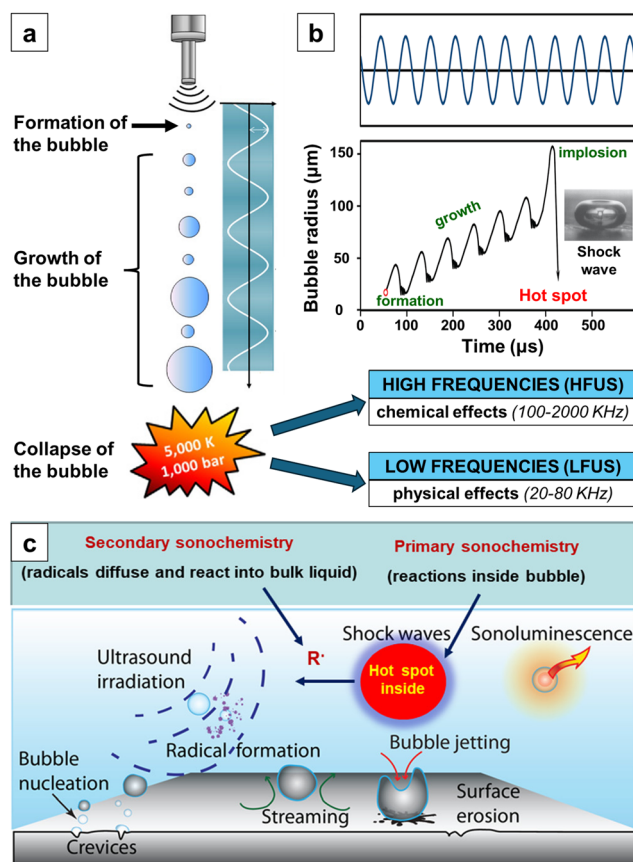


Fig. 2 (a) Cavitation events under ultrasonic irradiation, reproduced with permission from Chatel *et al.*⁴¹ Copyright 2016, Elsevier. (b) The change of bubble size during the cavitation, reproduced with permission from Xu *et al.*⁵¹ Copyright 2013, Royal Society of Chemistry. (c) Chemical and physical effects induced by acoustic cavitation, reproduced from an open access publication.⁴²

inertia of the surrounding fluid, propelling those radicals into the bulk solution (Fig. 2c). The propelled radicals can initiate further chemical reactions. Under an appropriate acoustic intensity, cavitation bubble implosion results in emission of a short flash of light (50–500 ps), a phenomenon known as sonoluminescence.^{37,38} Light emission with wavelengths between 200–800 nm suggests a high local temperature of approximately 5000 K at the cavitation site.³⁹ Suslick *et al.* investigated the sonoluminescence of a single bubble and reported that the energy released during cavitation bubble implosion is strong enough to induce chemical reactions.^{34,38} Reactions induced by this energy release include the homolytic dissociation of water to H^\bullet and $^\bullet\text{OH}$ radicals (water sonolysis) and the formation of NO_2^- by N_2 dissociation and its subsequent oxidation by O_2 or H_2O .³² The size (3–200 μm), lifetime (0.4 μs at 500 Hz, 10 μs at 20 kHz), and stability of cavitation bubbles depend on various factors, including the acoustic frequency, the acoustic intensity, physicochemical properties of the liquid, the presence of a dissolved gas, and the bulk solution temperature and pressure.^{36,40}

The radical composition inside a cavitation bubble depends on the gaseous atmosphere, the identity of the surrounding liquid, and the presence of dissolved solutes.^{32,33} For instance, high vapor pressure liquids or solutes can diffuse inside of the cavitation bubble where they are instantaneously pyrolysed. These pyrolysis reactions form additional radicals and co-products from radical recombination. Once these cavitation bubbles implode, the radicals are propelled into the solution where they can recombine (e.g. forming H₂O₂ and H₂, during water sonolysis) or oxidise the solutes.⁴² The chemical effect induced by sonochemistry can be significantly leveraged when it is controlled using heterogeneous catalysts. In some cases, the integration of sonochemical reactions with heterogeneous catalysts resulted in a reactivity increase by nearly a million-fold.³⁸ The ESI† summarises the general application areas of sonochemistry without the assistance of a catalyst. The next section is dedicated to more detailed applications of sonocatalysis, where the sonochemical reactions are facilitated by the presence of solid catalysts.

3. Sonocatalysis

3.1. What is sonocatalysis?

Sonochemical reactions can be classified into three types according to the nature of cavitation: homogeneous sonochemistry, heterogeneous sonochemistry, and sonocatalysis, which represents the intersection of the two (Fig. 3). In homo-

geneous sonochemistry, cavitation events occur in the liquid phase, generating active radicals that facilitate chemical reactions. Therefore, the key features of homogeneous sonochemistry are the chemical effects occurring in the liquid phase. In heterogeneous sonochemistry, the cavitation events occur in immiscible liquid–liquid or solid–liquid systems. The cavitation collapse generates shockwaves and microjets that enhance mass transport and accelerate chemical reactions. Sonocatalysis is a special application area where both the chemical and physical effects of ultrasound are leveraged to accelerate reactions in heterogeneous systems. In sonocatalysis, either phase of a liquid–liquid system, or the solid phase in a solid–liquid system acts as a catalyst to accelerate the chemical reaction occurring in the bulk liquid. The presence of this catalytic phase significantly enhances the rate of the reaction under ultrasonic irradiation, which has the potential to reach a million-fold enhancement in the reaction rate when compared to conventional process using the same catalyst in the absence of ultrasound.

Whether the physical or chemical effects of ultrasound are dominant depends on the operating conditions of the process. The most important parameter is the applied frequency of the ultrasound. At the lower frequency range (<100 kHz), physical effects dominate, while radical formation is often negligible (insert image in Fig. 3). These processes are called low frequency ultrasound (LFUS). In LFUS systems, the physical effects of cavitation, such as mixing, catalyst dispersion, and coke removal, are exploited for improving reaction rates. For example, LFUS has been used to accelerate the iron-catalysed oxidation of glucose by hydrogen peroxide. The formation of radicals increases when higher frequency ultrasound is used, but radicals' production decreases beyond a threshold value (Fig. 3). At elevated frequencies, cavitation bubbles collapse long before reaching their resonant size, thus decreasing the efficiency of active radical production. In addition, at higher frequencies, the energy supplied by ultrasonic irradiation is predominantly transformed into kinetic energy for molecular motion/vibration, resulting in the suppression of chemical effects. Consequently, the range from 200–500 kHz, called high frequency ultrasound (HFUS) is considered to be the best range for maximising the chemical effects of sonocatalysis. In the presence of nanoparticles, the formation of cavitation bubbles occurs preferentially on the nanoparticle surface *via* heterogeneous nucleation. In this way, radicals produced inside cavitation bubbles can be transferred to a nano-designed catalytic surface by the high-speed jets generated from the implosion of cavitation bubbles, offering promising tools for better control of the reaction selectivity.

Suslick *et al.* were the first to introduce the term of sonocatalysis in 1981.⁴³ In their study of olefin isomerisation under ultrasonic irradiation, they observed that the rate of isomerization of 1-alkenes on organometallic iron carbonyl compounds was 10⁵ times higher than that of traditional thermal reactions. Starting from 2015, sonocatalysis witnessed a renaissance in response to the urgent need for the development of new emerging green technologies that could address the

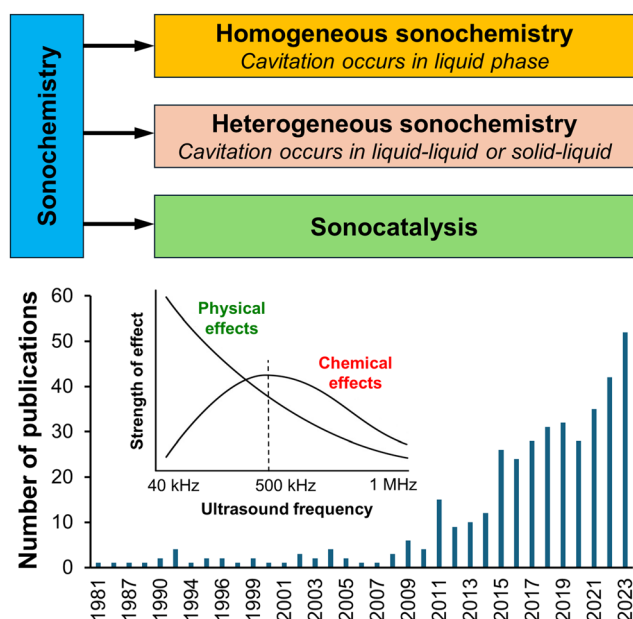


Fig. 3 Classification of sonochemical reactions (top) and number of publications with the keyword "sonocatalysis" in different years, from Scopus search, September 2024 (bottom). Insert image shows the contribution of two primary effects that enhance sonochemical reactions (physical effects by shear force and chemical effects by reactive radicals) at different ultrasound frequencies, reproduced with permission from McKenzie *et al.*²⁷ Copyright 2019, John Wiley and Sons.

United Nations Sustainable Development Goals. Since then, sonocatalysis has steadily received a great deal of attention from the global research community, as evidenced by the continuous upward trend in scientific publications (Fig. 3). In the following sections, we describe in more detail the recent success of sonocatalysis in wastewater treatment, medical therapy and biomass conversion. We focus on analysing the mechanism by which sonocatalysis outperforms conventional approaches in these applications to emphasise its potential in establishing a more sustainable society.

3.2. Sonocatalysis in wastewater treatment

The increasing accumulation of organic contamination in wastewater effluents, including organic dyes, antibiotics, pesticides, and pharmaceutically active compounds, poses a severe threat to the living ecosystem, biodiversity, and human health.^{44–47} The UN Sustainable Development Goals (SDG 6) states that ensuring accessibility to “clean and accessible water” will be crucial for the sustainable development of humans by 2030.⁴⁸ Therefore, it is an urgent task for the research community to develop efficient methods to tackle this challenge. Sonocatalytic approaches to wastewater treatment has attracted great interest as a highly effective and green alternative. Since those processes are usually carried out at ambient temperatures in water and use the catalyst to enhance the rate, yield, and selectivity, they align well with many principles of green chemistry, including the “Prevention”, “Design for energy efficiency”, “Safer solvent and auxiliaries”, “Catalysis”, “Inherently safer chemistry for accident prevention” and “Design for Degradation”. The recent integration of microfluidics sensing into sonocatalysis represents the “state-of-the-art” technology in environmental monitoring, allowing the precise control of sample collection and facilitating the rapid and highly sensitive detection of various analytes, further satisfying the principles “Real-time analysis for Pollution Prevention” of green chemistry.^{49–51} Excellent recent reviews in the applications of sonocatalysis in waste water treatment can be found by Wang *et al.*,⁵² Soni *et al.*,⁵³ Liu *et al.*,⁵⁴ Abdi *et al.*,⁵⁵ and Dhull *et al.*⁵⁶

There are two mechanisms by which sonocatalysts eliminate organic contaminants in wastewater: (1) direct contaminant degradation by the catalyst under ultrasound and (2) catalyst-enhanced sonolysis, which in turn decomposes contaminants (Fig. 4a). Jun *et al.* demonstrated these two mechanisms in the removal of methylene blue (MB) and acid blue 80 (AB) on the $\text{Ti}_3\text{C}_2\text{T}_x$ MXene catalyst under ultrasonic irradiation.⁵⁷ In the first mechanism, enhanced the mass transfer caused by cavitation bubble implosion facilitated the adsorption of methylene blue (MB) on the catalyst surface and significantly increased its degradation activity. While acid blue 80 (AB) could not be degraded directly using $\text{Ti}_3\text{C}_2\text{T}_x$ MXene catalysts under silent conditions (*i.e.*, without ultrasound), the presence of $\text{Ti}_3\text{C}_2\text{T}_x$ MXene catalysts enhanced the rate of water sonolysis, resulting in a higher density of ROS (H_2O_2 and $\cdot\text{OH}$ radicals), which in turn caused degradation. In order to make sonocatalysts more efficient in wastewater treatment, they are

engineered to have different morphologies that maximise their activity.

Ucar fabricated Cu-dopamine nanoflowers that exhibited high specific area and good activity for the degradation of methylene blue.⁶³ Dastborhan *et al.* prepared the nano-composite $\text{MoS}_2/\text{carbon}$ nano tubes in flower-like shapes as an efficient catalyst for the sonocatalytic degradation of hydroxy-chloroquine (Fig. 4b).⁵⁸ Similarly, Saravanakumar *et al.* produced sonocatalyst microrods of $\text{CoTiO}_3/\text{Ti}_3\text{C}_2\text{T}_x$ MXene that had high activity in bisphenol A (BPA) degradation (Fig. 4c).⁵⁹ Materials ranging from metal oxides,^{56,64} substrate-supported metal nanoparticles, metal sulphides,⁶⁵ metal phosphides, porous organic polymers, metal–organic frameworks (MOF)^{55,66} and MXenes⁶⁷ have been broadly developed for sonocatalytic water remediation. Recently the combination of different semiconductor phases with suitable valence band and conduction band potentials to construct a Z-scheme heterostructure is a research “hotspot” in sonocatalysis due to the fact that the presence of conductive channels, broaden the optical response range and intensify the redox driving force.^{68–71} Qiao *et al.* has managed to prepare the Z-scheme $\text{KTaO}_3/\text{FeVO}_4/\text{Bi}_2\text{O}_3$ nanocomposite (Fig. 4d), which showed excellent sonocatalytic activity for the degradation of antibiotic ceftriaxone.⁶⁰

In order to properly evaluate the performance of sonocatalysis, Qiu *et al.* collected experimental data from the sonocatalytic degradation of several microorganisms in water and plotted the rate constant of sonodegradation with and without the presence of the catalyst, Fig. 4e.⁴⁷ The database includes the sono-elimination of *Escherichia coli* (*E. coli*) at 39 kHz (Study 1),⁷² *Legionella pneumophila* at 36 kHz (Study 2),⁷³ *E. coli* at 36 kHz (Study 3),⁷⁴ and salicylic acid oxidation (Study 4) at 36 kHz on Al_2O_3 and TiO_2 catalysts. Fig. 6e shows that the sonocatalytic activity of Al_2O_3 is at least 10-fold higher than of ultrasound alone. Since Al_2O_3 does not have any catalytic activity for contaminant degradation without ultrasonic irradiation, the enhancement of sonocatalytic contaminant degradation was attributed to the catalyst enhancing cavitation. Fig. 6e also shows that the efficiency of TiO_2 is 1.4–3.8 times better than that of Al_2O_3 , and this was attributed to the synergistic effect between TiO_2 and ultrasound in generating higher density of ROS (enhanced cavitation by TiO_2) and in inducing the photo-thermal-catalytic effect (enhanced catalytic activity of TiO_2 by sonochemistry).⁴⁷ A more quantitative method to show the power of sonocatalysis involves benchmarking sonocatalytic efficiency against the effects of sonolysis, adsorption, and the summation of those two individual effects (adsorption + sonolysis), as in Fig. 4f.^{61,75} In the sonocatalytic degradation of sulfadiazine on a MXene-MOF catalyst, Ranjith *et al.*⁶¹ measured the rate constant of contaminant removal *via* catalytic adsorption (in the absence of ultrasound) and *via* sonolysis only (in ultrasound without catalysts), and *via* both contaminant removal methods combined. In Fig. 4f, the degradation rate coefficient obtained for sonocatalysis far exceeds the result obtained for all other experiments, highlighting the synergy between catalysts that are active under ultrasound and sonoly-

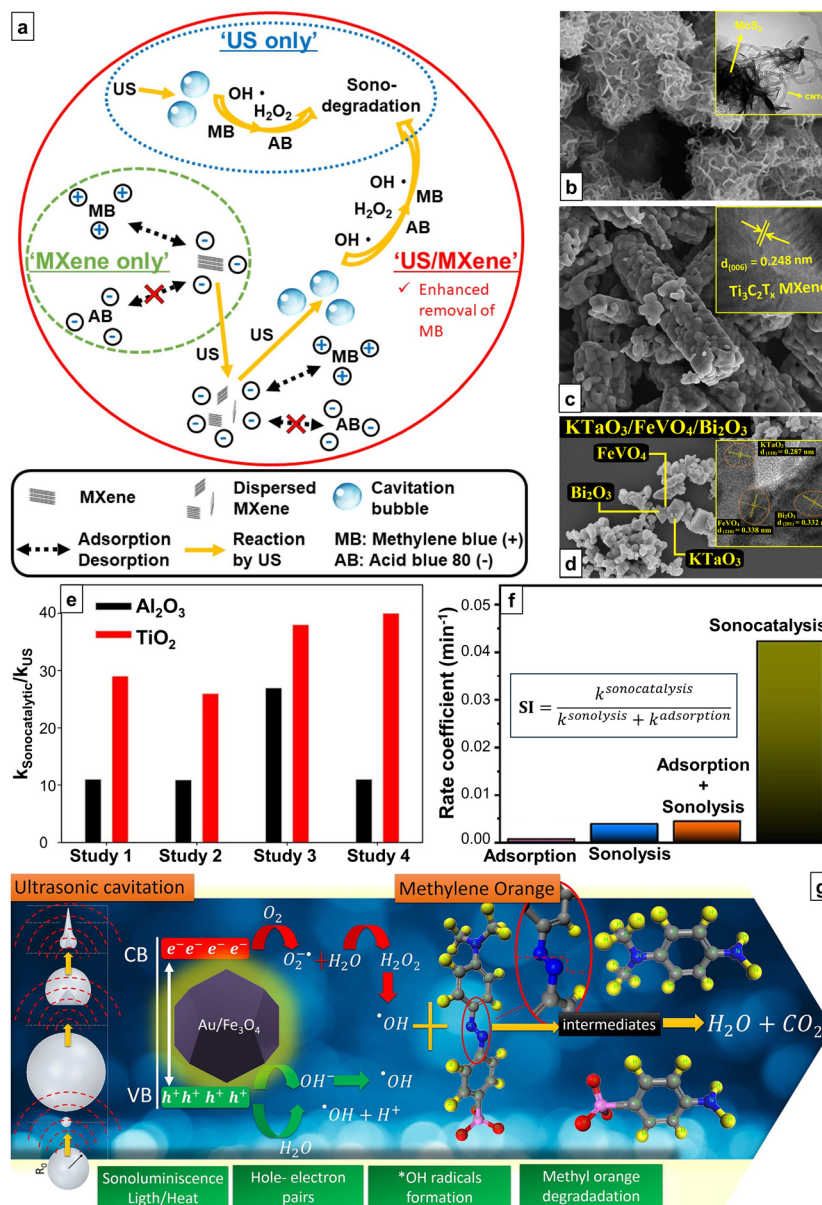


Fig. 4 (a) Mechanism for the sonocatalytic removal of organic dyes, reproduced with permission from Jun *et al.*⁵⁷ Copyright 2020, Elsevier. (b) SEM and TEM images of MoS₂/carbon nano tubes (CNT) nanoflower for the sonocatalytic degradation of hydroxychloroquine, reproduced with permission from Dastborhan *et al.*⁵⁸ Copyright 2022, Elsevier. (c) SEM and HR-TEM images of CoTiO₃-MXene microrods as sonocatalysts in bisphenol A degradation, reproduced with permission from Saravanakumar *et al.*⁵⁹ Copyright 2021, Elsevier. (d) SEM and HR-TEM images of Z-scheme KTaO₃/FeVO₄/Bi₂O₃ nanocomposite in the sonocatalytic degradation of ceftriaxone sodium antibiotic, reproduced with permission from Qiao *et al.*⁶⁰ Copyright 2019, Elsevier. (e) Enhancement of the sonocatalytic activities compare to the activities in silent conditions for the elimination of *E. coli* (Study 1), *Legionella pneumophila* (Study 2), *E. coli* (Study 3) and salicylic acid oxidation (Study 4) on Al₂O₃ and TiO₂, reproduced with permission from Qiu *et al.*⁴⁷ (f) Synergistic effect in the sonocatalytic degradation of sulfadiazine on MXene-MOF nanocomposite, reproduced with permission from Ranjith *et al.*⁶¹ Copyright 2018, Elsevier. (g) Sono-degradation mechanism of methyl orange by Au/Fe₃O₄ nanoparticles, reproduced with permission from Ruiz-Baltazar.⁶² Copyright 2021, Elsevier.

sis. A synergy index, which is computed using the formula in Fig. 4f, is a convenient metric for expressing the synergy of sonocatalysis, which can be used to benchmark the performance of different catalysts for the sono-degradation of the same contaminant.

Finally, efforts have been made to obtain a more detailed understanding of the sonocatalytic mechanism for water treat-

ment *via* molecular modelling. Ruiz-Baltazar *et al.*⁶² conducted a comprehensive characterization of Au/Fe₃O₄ catalysts and proposed a mechanism for the sonodegradation of methyl orange using computational simulations (Fig. 4g). Their results showed that cavitation bubble implosion generates sufficient light and heat (*via* sonoluminescence) to create electron-hole pairs in the conduction band (CB) and the valence

band (VB) at the interface between Au and Fe₃O₄. These electron-hole pairs were active in facilitating water sonolysis, producing a high density of $\cdot\text{OH}$ radicals, which are essential for methyl orange degradation, Fig. 4g. Experimental results showed that an excellent sonocatalytic efficiency of 91.2% was obtained after a short reaction time of 15 min. This detailed mechanistic understanding of sonocatalyst operation is helpful in aiding the design of other sonocatalytic wastewater treatment methods in the future.

3.3. Sonocatalysis in medical therapy

Another important application area of sonocatalysis is medical therapy. This application addresses the **UN Sustainable Development Goal 3** (Good health and well-being), ensuring “*healthy lives and promoting well-being for all at all ages*”. In this field, sonocatalysts are being applied in cancer therapy, antibacterial therapy, and therapeutic nanomedicine. Previously, sonochemistry was used to enhance the penetration range and drug efficiency in photodynamic therapy, which is a well-developed stimuli-responsive and non-invasive method for tumour treatment.^{4,5} In photodynamic therapy, a photo-responsive drug is activated with photoenergy, releasing active radicals that kill cancer cells with minimal side effects. However, the penetration depth of light in photodynamic therapy is up to 1cm and is therefore only able to access skin and prostate cells. Consequently, photodynamic therapy is not effective to treat cancer cells for major internal organs (e.g., liver, pancreas, kidney) which would require a penetration depth larger than 7 cm. On the other hand, the penetration depth of radiation therapy is much larger than photodynamic therapy, allowing it to be applied in treating deeper tumour sites. However, the downside is that the strength of the radiation is too strong, causing severe damage on neighbouring normal tissues. The penetration depth of sonotherapy (therapy using ultrasound) is ~ 10 cm, which is ideal for accessing the major organ tissues without using harmful radiation. Recently, the application of sonocatalysis in medical therapy, called sonodynamic therapy (SDT), has been receiving a lot of attention from researchers, especially in cancer treatment, both as an individual strategy or in cooperation with photodynamic therapy. Cancer is considered a global health challenge, and it is among one of the most common threats to human health. The risk of cancer is intensified due to the fast-changing climate and intensive industrialization that drastically change our living environments. Therefore, the development of sustainable technologies, like sonodynamic therapy, that are highly effective for cancer treatment are vital to the improvement of human health. The applications of sonocatalysis in medical therapy also satisfy principles of green chemistry such as “*Atom economy*”, “*Designing Safer Chemicals*”, “*Design for energy efficiency*”, “*Safer solvent and auxiliaries*”, “*Catalysis*” and “*Inherently safer chemistry for accident prevention*”.

Due to the complex reactions occurring inside of cancer cells, the detailed mechanism for the effectiveness of sonocatalytic therapy is not yet fully understood. Despite this, extensive efforts are being made to gain more insight into the pro-

cesses occurring during catalytic sonotherapy. It is widely proposed that therapy mechanisms including sonocatalysis function *via* mechanical, chemical, and thermal effects. Mechanical effects, such as microstreaming, microjets, and shockwaves, are produced by acoustic cavitation and act on cell structures, causing necrosis or cell death. Thermal effects result from the release of heat stored inside a bubble during implosion, activating thermal necrosis of the tumour tissues located in proximity to the cavitation bubbles. However, the most impactful factor of sonocatalytic therapy is its chemical effect, stemming from the production of highly active radical species. Reactive oxygen species (ROS) generated during bubble collapse can destroy tumour cells through cell apoptosis. However, the presence of these ROS triggers two subsequent feedback reactions from the tumour microenvironment (TME): hypoxia which suppresses the production of ROS and an over-expressed glutathione (GSH) which consumes the existing ROS, resulting in decreased therapeutic efficacy. These two feedback reactions and the high level of H₂O₂ accumulated from water sonolysis can have the undesired effect of actually promoting the growth and metastasis of cancer cells. After periods of sufficiently long exposure, this might eventually cause the tumour cells to become drug and immune resistant. Therefore, another important role of the catalyst is to regulate the TME to reduce these risk factors and enhance the efficiency of sonotherapy. Designing sonocatalysts that generate a high density of ROS and are able to tune the TME is vital to the improvement of sonocatalytic therapies.

Liu *et al.* succeeded in preparing ultrathin-FeOOH-coated MnO₂ nanospheres (denoted as MO@FHO) that were used as bifunctional sonocatalysts that both promoted ROS generation and inhibited the TME.⁷⁶ Fig. 5a presents the anticancer mechanism of this material. Fig. 5b shows the *in vivo* experimental efficiency of tumour treatment on mice. MnO₂ acts as the catalytic center, and its catalytic activity is accelerated by the FeOOH phase, jointly producing a high density of ROS, including $\cdot\text{OH}$, $\cdot\text{O}_2^-$, and singlet $^1\text{O}_2$ species, under ultrasonic irradiation. In addition, the interaction between the MnO₂ core and the FeOOH shell created intrinsic multivalent metal ions at the interfacial zone of MO@FHO that catalysed H₂O₂ decomposition to relieve tumour hypoxia and reduce the GSH (Fig. 5a). *In vitro* experiments showed that the ROS yield of MO@FHO under ultrasound was much higher than compared to the control case without the catalyst. The MO@FHO was also able to disrupt the metabolic equilibrium of the cells and regulate the TME. *In vivo* tests on mice with MBA-MD-231 breast cancer cell indicated a significant inhibition of tumour growth (Fig. 5b). Alleviation of tumour hypoxia was confirmed by immunostaining assays analysing the indicators HIF-1 α and VEGF. This study created a strategy for designing highly effective nano-catalysts for sonotherapy that are active in ROS generation and are capable of regulating the TME.

The light (*via* sonoluminescence), heat (*via* solvent pyrolysis) and piezoelectric potential (*via* piezoelectric effect) generated during cavitation events also enhance the activity of sonocatalysts. In particular, bubble collapse has the ability to

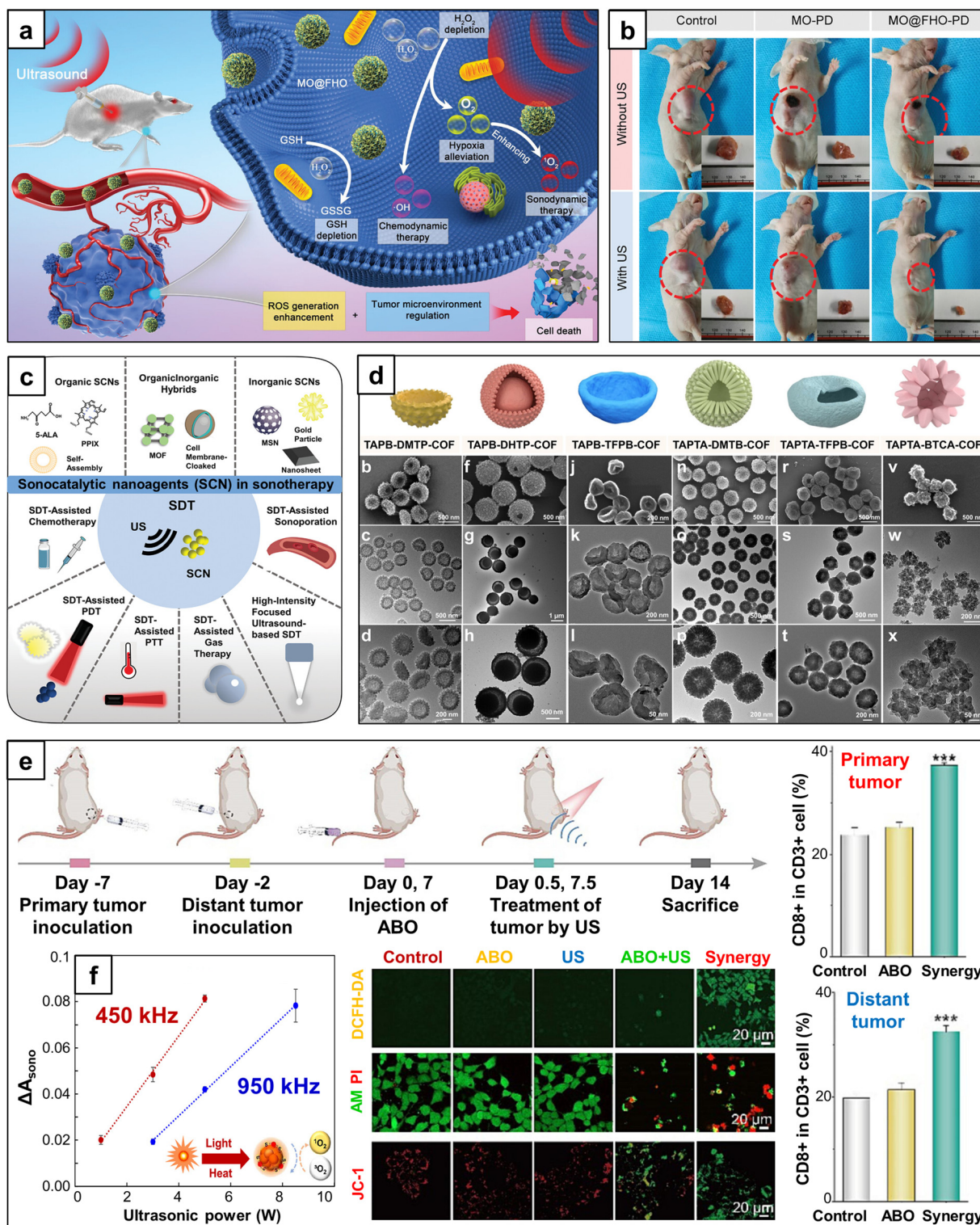


Fig. 5 (a) Mechanism of cancer treatment and (b) images of the tumours present in mice during sonotherapy treatment with MnO₂@FeOOH nano-spheres (called MO@FHO), reproduced from an open access publication.⁷⁶ (c) Sonocatalyst nanoagents (SCN) and their corresponding sonodynamic therapy (SDT) applications, reproduced with permission from Feng *et al.*⁷⁷ Copyright 2023, John Wiley and Sons. (d) Different morphologies of covalent organic frameworks (COF) synthesised for sonotherapy, reproduced with permission from Liu *et al.*⁸⁰ Copyright 2023, John Wiley and Sons. (e) In vivo treatment on Au-Bi₂O₃ nanoheterojunction sonocatalysts (called ABO), reproduced with permission from Chen *et al.*⁸¹ Copyright 2024, Elsevier. (f) Sonotherapy efficiencies at different applied ultrasound frequencies and powers, reproduced with permission from Yagi *et al.*⁸² Copyright 2022, American Chemical Society.

modify the electronic properties of the catalytic material by changing its bandgap and/or improving the separation of electron–hole pairs, increasing the production of ROS. As a result of these effects, the sonocatalytic nanoagents (SCNs) used in therapeutic applications are also called “sonosensitisers”. Advanced SCNs with high therapy efficiency are constructed from a wide range of materials, including organic materials (*e.g.*, phenothiazine compounds, fluoroquinolone antibiotics, porphyrins, and xanthenes), inorganic materials (*e.g.*, noble metal nanoparticles, transition metal oxides, sulphides, carbon-based nanomaterials, quantum dots, piezoelectric materials, and Z-scheme and S-scheme heterostructures), and organic/inorganic hybrid nanoparticles (*e.g.*, metal organic frameworks (MOFs), zeolitic imidazolate framework (ZIFs), and covalent organic frameworks (COFs)). The efficiency of sonocatalytic nanoagents (SCN) in generating ROS and their effect in TME regulation can be greatly enhanced by combining SDT with other techniques. These techniques incorporating SDT include high-intensity focused ultrasound-based SDT, SDT-assisted sonoporation, SDT-assisted photothermal therapy (SDT-PTT), SDT-assisted chemotherapy (SDT-CDT), SDT-assisted gas therapy, and SDT-assisted photodynamic therapy (SDT-PDT) (Fig. 5c).⁷⁷ The recent development of novel sonocatalytic nanoagents and DFT-assisted therapy processes are summarised in excellent reviews by Son *et al.*,⁷⁸ Feng *et al.*⁷⁷ and Yang *et al.*⁷⁹

Among the three types of SCNs shown in Fig. 5c, small organic SCN molecules are traditionally used for sonotherapy. However, disadvantages, such as low stability, weak tumour enrichment abilities, inhomogeneous distribution, and low efficacies in generating ROS, hindering their wider application. In recent years, the self-assembly of organic SCNs with biocompatible components to form nanosystems emerged as a promising method to address the above problems, improving sonotherapy efficiency. Excellent candidates for SDT are hybrid organic/inorganic materials (MOFs, ZIFs and COFs), which are crystalline and porous materials with large surface area, high stability, and tunable electronic features. The morphology of these hybrid organic/inorganic SCNs is of particularly importance for sonotherapy applications since it affects the delivery of the SCN into the tumour cells and the generation of the ROS. Great efforts have been made in literature to control the synthesis of hybrid organic/inorganic SCNs to achieve a desired morphology. Liu *et al.* developed a facile two-step procedure to synthesise a library of hollow COFs with diverse nanostructural morphologies, including the bowl-like, yolk-shell, nanosphere, nanorods, capsule-like, and flower-like structures (Fig. 5d).⁸⁰ Each of these morphologies has its own targeted application corresponding to a particular sonodynamic cancer therapy.⁸³

Inorganic materials compose one third of SCNs and are the most widely used material in SDT, owing to their versatile compositions, excellent stability, high activity, and selectivity. Usually, inorganic catalysts in SDT are heterostructures built from two solid phases. The activity and electronic properties of these materials can be fine-tuned *via* doping, alloying,

functionalization or *via* metal/support interactions. This offers great flexibility for fabricating highly efficient catalysts for targeted applications in SDT. Chen *et al.* prepared nanoflowers of the Au-Bi₂O₃ nanoheterojunction (called ABO) for the therapy of 4T1 tumour cells.⁸¹ The plasmonic resonance effect between metallic Au and semiconductor Bi₂O₃ phases induced the separation of electrons and holes of ABO under ultrasound, promoting ROS generation and enhancing photothermal effects of the Bi₂O₃ phase. Elevated ROS generation subsequently disrupted the redox balance of tumour cells by consuming their intratumoral overexpressed glutathione. Combined, these effects cooperatively induced immunogenic cell death, which was reflected in the *in vitro* therapeutic test *via* a 2',7'-dichlorodihydrofluorescein diacetate (DCFH-DA) probe, calcein acetoxymethyl ester (Calcein-AM)/propidium iodide (PI) staining, and a JC-1 assay in 4T1 cells (Fig. 5e). *In vivo* antitumour therapy was also conducted on mice and the combination of ABO + US was responsible for inhibiting the growth of both primary and distant tumours (Fig. 5e), emphasising the efficiency of this material in sonocatalytic therapy treatments.

Applied ultrasonic frequency and power are the most important parameters for sonocatalytic cancer treatment since they greatly influence the generation of ROS, Fig. 5f.⁸² There is a need to optimise the ultrasonic frequency to find the conditions that maximise the ROS yield (often at moderate frequency around ~500 kHz) and also the penetration depth, which decreases as a function of increasing frequency. The best practice is to choose the frequency that corresponds most strongly to the type of tumour cells under treatment. Despite its potential, sonocatalytic therapy is still in an early technological readiness level (TRL) or laboratory stage and has not been clinically tested or approved for cancer treatment. Extensive development in this field is still needed to connect experimental observations with clinical applications. More interdisciplinary studies will be required to fully understand the mechanism underlying sonocatalytic therapy processes. Ultimately, the goal is to design novel sonodynamic nanoagents with better biocompatibility and higher catalytic efficiency, and to evaluate side effects and long-term toxicity before the scale-up.

3.4. Sonocatalysis in biomass conversion

According to the United Nations, the world population will grow to 9.8 billion by 2050.⁸⁴ This population growth will drastically increase the demand for energy, food, and chemicals. Sustainably meeting these demands while protecting our environment has become one of the highest priorities.⁸⁵ The progressive incorporation of renewable biomass resources, including lignin, carbohydrates, and polysaccharides, in the chemical industry is a revolutionary transition towards building a green circular and sustainable chemical supply chain.^{86–93} This contribution is driven by the carbon-neutral nature of biomass and its huge capacity to produce a wide range of fuels and chemicals that are essential for human life. However, controlling the selective conversion of the polyfunc-

tional substrates comprising biomass is a grand challenge, and currently limits the potential of biomass transformation into high value-added specialty chemicals, such as bio-based products. To address this selectivity challenge and facilitate biomass conversion, a new concept of assisted catalysis has emerged, wherein chemical reactions are driven at room temperature by external triggers like electrical potentials,⁹⁴ photons,^{48,95,96} plasma,^{94,97} and ultrasound.^{98,99}

Among these driving forces, ultrasound, in particular, is experiencing a renaissance. At high applied frequencies, ultrasound-generated radicals can participate in chemical reactions. Paquin *et al.* used ultrasound at a frequency of 170 kHz to significantly improve the cellulose oxidation to carboxylic acids.¹⁰⁰ Amaniampong *et al.* found that the carbohydrate concentration had a strong effect on the mechanism of the

radical-driven conversion of biomass substrates (Fig. 6a).¹⁰¹ The conversion of glucose under 550 kHz ultrasonic irradiation occurred *via* a pyrolysis-like mechanism at the liquid-bubble interface. Levoglucosan was generated *in situ* as the key intermediate species and ultimately led to the formation of alkylpolyglycosides (APGs) as the main products, which have important applications in the food, cosmetics, detergent, and pharmaceutical industries.¹⁰² The key advantage of ultrasound-assisted glucose conversion to APGs is its reaction at 40 °C without the use of (bio)catalysts as in conventional methods, therefore preventing the degradation of carbohydrates. In contrast, at concentrations lower than 10 wt%, glucose is oxidised by $\cdot\text{OH}$ radicals produced from water sonolysis, resulting in the formation of either gluconic or glucuronic acid under different gas atmospheres.²⁸ However, control-

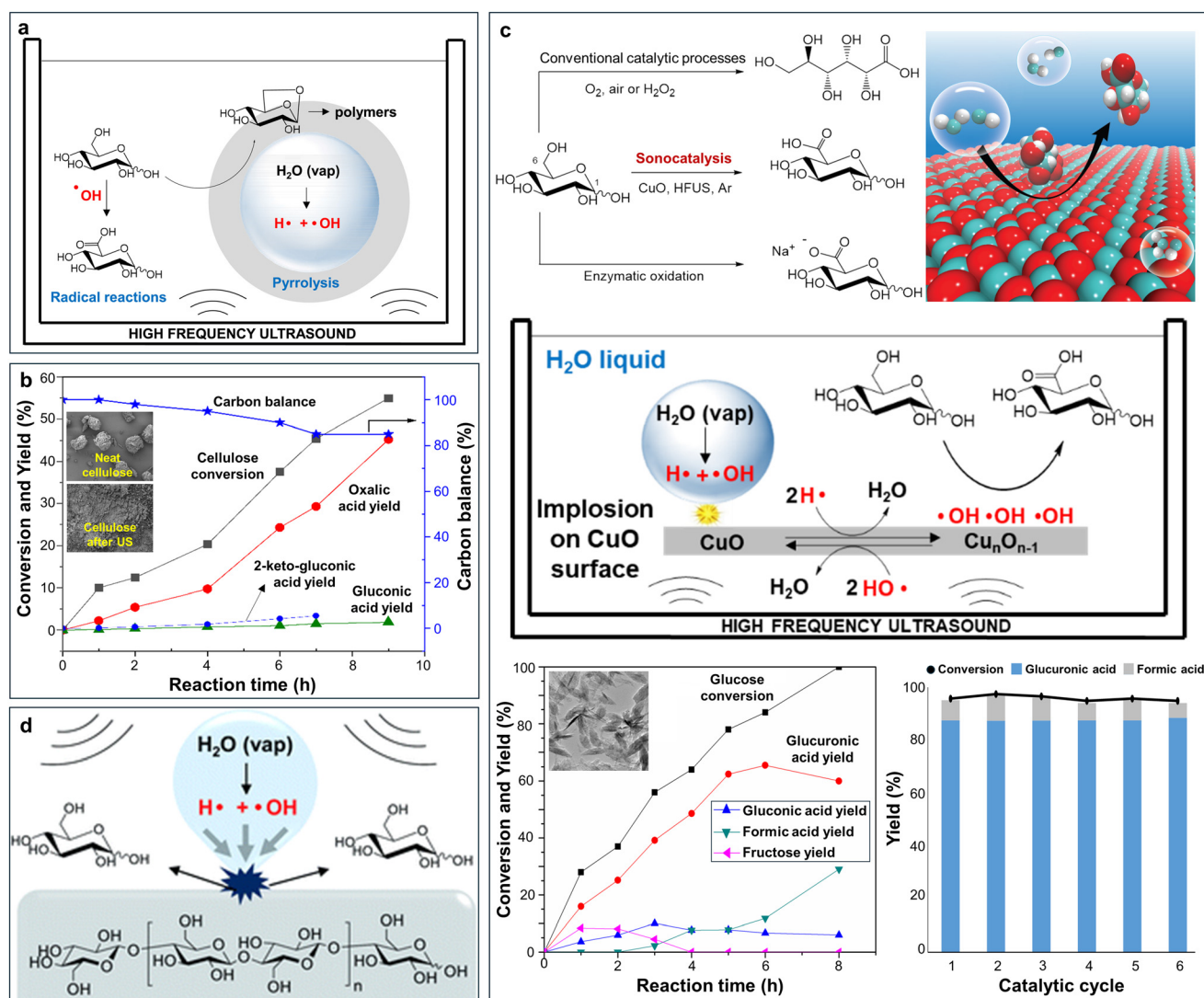


Fig. 6 (a) Mechanisms and products of glucose conversion under ultrasonic irradiation at different conditions, reproduced with permission from Amaniampong *et al.*¹⁰¹ Copyright 2020, Elsevier. (b) Cellulose sono-conversion on Au/Fe₂O₃ catalysts, reproduced with permission from Amaniampong *et al.*⁹⁹ Copyright 2022, Royal Society of Chemistry. (c) Synergistic effect between CuO and HFUS in achieving selective glucose oxidation, reproduced with permission from Amaniampong *et al.*⁹⁸ Copyright 2019, American Chemical Society. (d) Complete depolymerization of cellulose to glucose under HFUS, reproduced from an open access publication.¹¹²

ling the rate and optimising the selectivity of the reaction under high frequency ultrasonic irradiation remain significant technological challenges. Therefore, in the absence of catalysts, the homogeneously generated radicals of high frequency ultrasound (HFUS) are mainly used for the total oxidation of aqueous pollutants.

In the presence of nanoparticles, the formation of cavitation bubbles occurs preferentially on the nanoparticle surface *via* heterogeneous nucleation. In contrast to symmetrical cavitation bubble implosion in a homogeneous solution, the asymmetrical implosion of cavitation bubbles on a solid surface generates high-speed jets of liquid directed towards the surface. The enhanced mass transfer resulting from the high-speed jets is an effective means to concentrate radicals on the surface of catalysts, which allow them to participate in chemical reactions. So far, this strategy has mostly been applied in LFUS (<20 kHz) systems, where radical formation is negligible and the physical effects of cavitation (*e.g.*, mixing, catalyst dispersion, and coke removal) are dominant for improving reaction rates.^{103–106} For instance, Rinsant *et al.*¹⁰⁷ and Napoly *et al.*¹⁰⁸ used LFUS (20 kHz) to accelerate the iron-catalyzed oxidation of glucose by hydrogen peroxide. Sarwono *et al.*¹⁰⁹ and Marullo *et al.*¹¹⁰ obtained a high conversion rate when using an ionic liquid with HY zeolite catalysts to convert a wide range of biomass substrates (glucose, fructose, sucrose, cellulose, and raw bamboo biomass) to a promising platform chemical, 5-hydroxymethylfurfural (HMF), under LFUS at 20 kHz. The transformation of biomass-derived platform chemicals (such as HMF, vanillyl alcohol, and glyoxal) to higher value-added chemicals by sonocatalysis was also reported.^{105,111}

Sonocatalysis is also effective for the conversion of lignin which constitutes 15–20% of lignocellulosic biomass.^{113–115} Second generation lignocellulosic biomass, consisting of lignin, cellulose, and hemicellulose, is the largest renewable source of carbon.¹¹⁶ The introduction of these feedstocks in the chemical industry promotes the production of environmentally friendly chemicals and a wide range of sustainable consumer products. Du *et al.* transformed lignin to bio-oil using a phosphotungstic acid (PTA) sonocatalyst under ultrasonic irradiation at 35 kHz.^{117–119} In this study, 94.79% lignin depolymerization was achieved, with bio-oil composing 90.6% of the product yield and the remainder being a small quantity of phenolic monomers. Due to the low quantity of radical species produced in low frequency ultrasound, H₂O₂ typically needs to be added into the reactant mixture to provide a higher density of ROS,^{107,120,121} which makes the process less “green”. However, if catalysts can be designed so that they generate higher amounts of ROS species, biomass conversion can be facilitated even at LFUS conditions. Recently, Amaniampong *et al.* carried out the conversion of cellulose under LFUS on a catalyst composed of Au nanoparticles on a Fe₂O₃ support (Au/Fe₂O₃). They observed a 45% yield of oxalic acid, which is an industrial platform chemical with applications for polymers, leather manufacturing, celluloid production, and the synthesis of pharmaceutical intermediates

(Fig. 6b).⁹⁹ The presence of ultrasonic energy was vital for fragmenting the cellulose particles (inserts in Fig. 6b), cleaving the β-1,4 glycosidic bonds and simultaneously generating H₂O₂ *via* cavitation events. The generated H₂O₂ was subsequently activated at interfacial sites of the Au/Fe₂O₃ catalyst to produce reactive surface atomic oxygen species (O*) that were responsible for cellulose oxidation. Most applications of LFUS in sonocatalysis primarily enhance the reaction rates, while controlling the reaction selectivity under LFUS is more challenging.

On the other hand, sonocatalysis using HFUS provides a better alternative for improving both the reaction rates and the reaction selectivity of biomass conversion. This is due to the high density of active radical species produced during rapid cavitation and simultaneously transferred to the catalyst surface. With an appropriate catalyst design, the affinity of the radicals to the catalyst surface can be increased. Tailoring these relative affinities can reduce parasitic reactions (*e.g.* unselective free radical annihilation) in the bulk solution, offering better control of the selectivity of the reaction towards the formation of a desired product. Recent progress has been made in the field of biomass conversion based on applying sonocatalysis under HFUS.^{98,122} In 2019, guided by density functional theory (DFT) calculations, Amaniampong *et al.* reported that using a CuO nanoleaf catalyst under HFUS significantly increased the selectivity of glucose oxidation to glucuronic acid, which is an important pharmaceutical intermediate in the production of drugs for blood coagulation inhibitors, and antioxidants (Fig. 6c).⁹⁸ Under optimised conditions, a total yield of 88% glucuronic acid was achieved. The catalyst remained highly stable even after 6 catalytic cycles (Fig. 6c). This discovery represents a significant advancement since the conventional catalytic oxidation of glucose usually produces gluconic acid, a lower-value product used to make industrial cleaners, *via* oxidation of the anomeric position.^{123,124} Before this study, the heterogeneously catalyzed selective oxidation of glucose to glucuronic acid (oxidation *via* the C6 position) was not possible. This work also highlighted the importance of optimising the size of CuO nanoleaves for sonochemistry under HFUS. The efficient transfer of radicals from cavitation bubbles to the catalyst surface required nanostructured CuO with a specific size and morphology.⁹⁸ Recently, Bahry *et al.* reported the highly selective demethylenation of benzyl alcohol, a biomass-derived intermediate compound, on CuO catalysts at 578 kHz and an acoustic power of 0.11 W mL⁻¹.¹²² The use of HFUS changed the selectivity of the products from benzaldehyde, typical for conventional thermal catalytic reactions, to phenol. Sonocatalysis using HFUS can even be applied for the conversion of raw cellulose, since it was reported that cellulose was selectively depolymerised to glucose by ultrasonic irradiation in water at high ultrasonic frequencies (Fig. 6d).^{86,87,112} These discoveries pave the way toward effectively fine-tuning reaction selectivity in the transformation of biomass-derived feedstocks to high value-added specialty chemicals, enabling access to chemicals that are generally not synthesizable by conventional routes. This approach

opens new pathway for sonocatalysis aligning with green chemistry principles “*Use of Renewable Feedstocks*” and “*Reduce Derivatives*”. Recent successes in synthesising nanocatalysts *via* sonochemical approach as the “green method” with high control over morphology and particle size with superior activity and stability (ESI†) further facilitate the principle of “*Less Hazardous Chemical Syntheses*”,¹²⁵ enabling the applications of sonocatalysis in biomass conversion to satisfy 10 over 12 principles of green chemistry, except “*Design for Degradation*” and “*Real-Time Analysis for Pollution Prevention*”.

3.5. Sonocatalysis in other green and sustainable chemistry applications

With the increasing accumulation of CO₂ and greenhouse gas emissions in the atmosphere causing a severe impact on climate, significant efforts are being made in the field of CO₂ reduction, decarbonization, and the development of carbon-free, renewable energy sources to replace fossil fuels. This section introduces recent approaches using sonocatalysis for H₂ production, CO₂ activation, and N₂ fixation. These approaches are typical case studies of how sonocatalysis can contribute to green chemistry by addressing climate change and promoting renewable sustainability. The activation of CO₂ is the first step for its utilisation, which in turn contributes to the reduction of CO₂ levels in the atmosphere.^{126,127} H₂ is a high-density fuel source and its production is considered a promising energy alternative since its combustion only yields water. Therefore, producing H₂ from green methods will help to promote the development of a “hydrogen economy”.^{128–132} N₂ fixation is a chemical process that activates molecular N₂ and converts it to other useful nitrogenous compounds, like ammonia. Currently, N₂ fixation is a highly energy intensive process that produces a large amount of CO₂ emissions. Therefore, developing greener method of N₂ fixation *via* sonocatalysis can also help to address climate change.^{133,134} Sonocatalysis accelerates those reactions at near-ambient temperatures without external additives, reducing the reaction induction periods and the number of reactions steps and finally directing the reactions to alternative pathways.

Under the influence of ultrasound, cavitation events occur that result in the production of [•]H and [•]OH radicals *via* water sonolysis. These radicals diffuse into the bulk liquid and partially recombine to form H₂ and H₂O₂, which can be measured experimentally. While the ROS generated from cavitation events are used as oxidising agents in sonocatalysis, the generation of gaseous hydrogen has received less attention from researchers. However, the production of H₂ during sonochemistry has received more attention since the perspective article by Rashwan *et al.* was published in 2019,¹³⁵ coining the term “sono-hydro-gen”. The same term was later used in the review article “The Sono-Hydro-Gen process (Ultrasound induced hydrogen production): Challenges and opportunities”.¹³⁶ These papers highlighted the potential of H₂ production *via* sonochemical processes in comparison with thermochemical, electrochemical, photobiological, and photoelectrochemical

technologies.^{136,137} The key reactions for H₂ production in sono-hydro-gen are:



wherein reaction (1) is water sonolysis and reactions (2) and (3) are the two main reactions responsible for producing H₂. Merouani *et al.* measured the chemical kinetics of water sonolysis in combination with bubble dynamics in an acoustic field. They reported that reaction (3) contributed to 99.9% of hydrogen production,¹³⁸ while reaction (2) only had a minor contribution and occurred at the interface of the bubble.¹³⁹ With sono-hydro-gen, the average hydrogen production rate is only ~0.8 μM min⁻¹, which is much lower than the level applicable for commercialization, thus further improvements in performance and efficiency are necessary.^{136,140,141}

Catalysts can be used to improve the H₂ production in a sono-hydro-gen process. In fact, utilising catalysts to enhance sonocatalysis-mediated hydrogen therapy has been reported recently.^{142–144} Yuan *et al.* used Pt-Bi₂S₃ catalysts to facilitate the hydrogen evolution reaction (HER) under ultrasonic irradiation, which subsequently induced mitochondrial dysfunction and disrupted the tumour’s antioxidation defence system, leading to cell death.¹⁴² However, the use of sonocatalysis for direct H₂ production is still in its infancy, despite some promising recent studies. Wang *et al.* reported that Au/TiO₂ sonocatalysts were active for promoting water sonolysis and producing H₂ under ultrasonic activation at 40 kHz.¹⁴⁵ Qi *et al.* carried out sonocatalytic H₂ production on flower-like Co₄N nanowires. The engineered nanostructures with rich nitrogen-vacancies led to stronger adsorption of the [•]H radicals generated by cavitation on the surface of the catalysts, facilitating H₂ production (Fig. 7a).¹⁴⁶ Ultrasonic irradiation at 40 kHz and 100 W achieved a H₂ production rate of 28.5 μmol g⁻¹ h⁻¹ (Fig. 7b), while only a trace amount of H₂ was detected without ultrasound.¹⁴⁶ Pollet *et al.* recorded the HER on a Pt catalyst with a high-speed camera (Fig. 7c) and observed a H₂ production efficiency increase of 250% under ultrasound.¹⁴⁷ Foroughi *et al.* also reported that the HER was facilitated on RANEY®-Ni catalysts under ultrasonic irradiation at 408 kHz (Fig. 7d).¹⁴⁸ Zhang used BaTiO₃ nanofluid catalysts under ultrasound to achieve a high rate of 270 mmol h⁻¹ g⁻¹ for H₂ evolution.¹⁴⁹ These studies illustrate the promising role of sonocatalysis in H₂ production.

Activation of CO₂ is the first step in reutilising CO₂ to reduce its atmospheric concentration. The bond energy in CO₂ is extremely stable at ~800 kJ mol⁻¹,¹⁵² therefore it only can be activated under high energy input or using extremely active catalysts. Recently, Islam *et al.* reported that the conversion of CO₂ to hydrocarbons (*i.e.*, the Sabatier reaction) was feasible in the presence of ultrasonic irradiation and this discovery was subsequently named the “Islam–Pollet–Hihn process”.¹⁵³

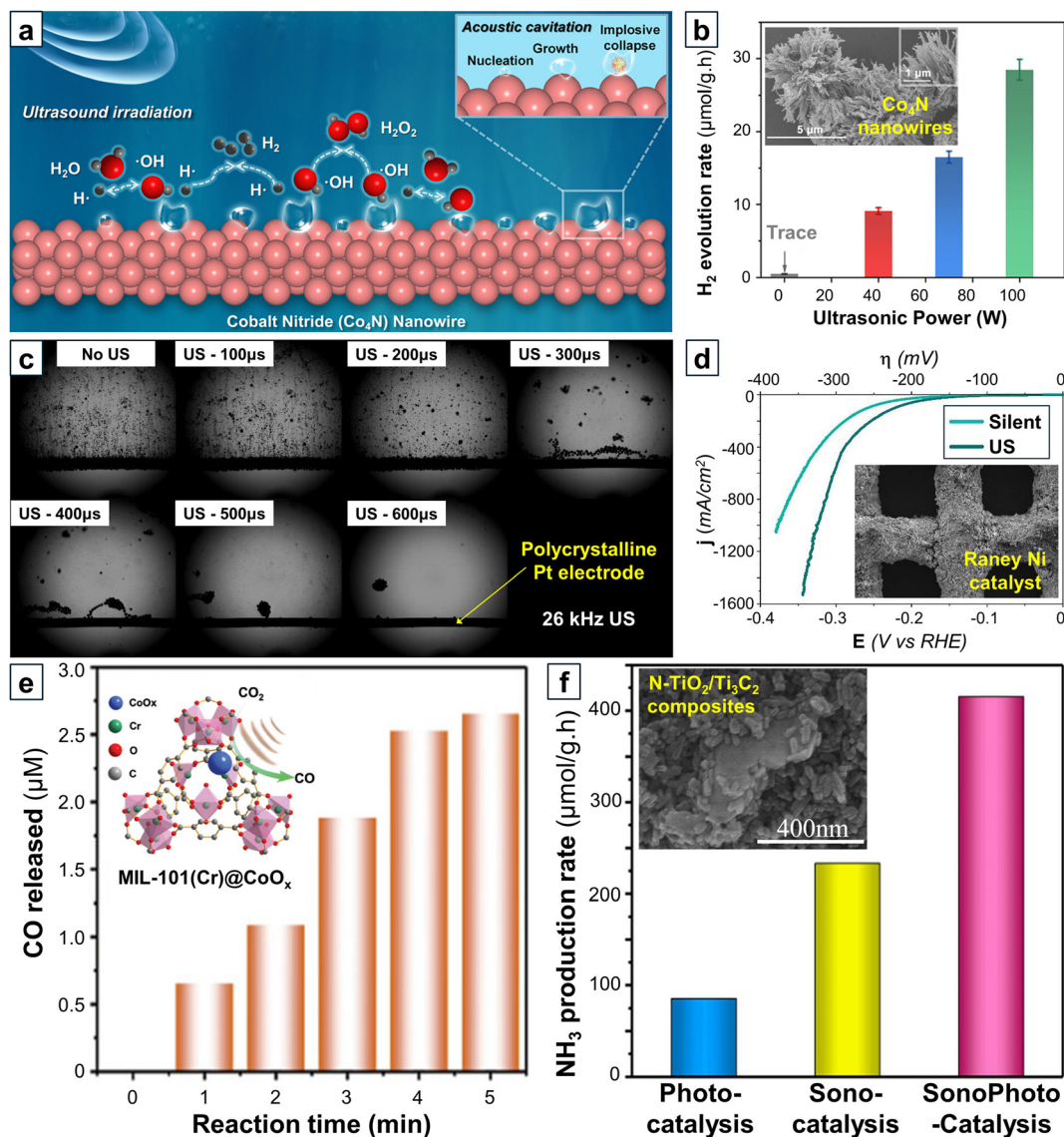


Fig. 7 (a) Sonocatalytic mechanism of H_2 production and (b) influence of ultrasonic power on the H_2 production rate in the presence of catalytic Co_4N nanowires, reproduced with permission from Qi *et al.*¹⁴⁶ Copyright 2023, American Chemical Society. (c) Hydrogen evolution reaction (HER) on a Pt wire with and without ultrasound, reproduced with permission from Pollet *et al.*¹⁴⁷ Copyright 2020, Elsevier. (d) HER on a RANEY®-Ni catalyst under silent conditions (without ultrasound) and under ultrasonic irradiation at 408 kHz, reproduced from an open access publication.¹⁴⁸ (e) Amount of CO produced *via* CO_2 sono-reduction using MIL-101(Cr)@ CoO_x catalysts, reproduced with permission from Zhang *et al.*¹⁵⁰ Copyright 2024, John Wiley and Sons. (f) NH_3 formation rate *via* sonocatalysis, photocatalysis, and sonophotocatalysis using composite N- $\text{TiO}_2/\text{Ti}_3\text{C}_2$ catalysts, reproduced with permission from Ding *et al.*¹⁵¹ Copyright 2024, Elsevier.

Using a sonoreactor coupled with a 488 kHz ultrasonic transducer, Islam *et al.* obtained the large amount of CO and a mixture of hydrocarbons, including CH_4 , C_2H_4 and C_2H_6 , as the main products. This study, reported in 2022, demonstrated that sonochemical activation could be used to convert CO_2 , but the reaction efficiency was low and left a lot of room for improvement.¹⁵³ It is probable that the process could be made more efficient through the introduction of catalysts. The concept of sonocatalysis in CO_2 activation has already been reported in ultrasound-assisted sonodynamic gas cancer therapy.^{150,154} Zhang *et al.* synthesised nanocatalysts by inte-

grating CoO_x into metal-organic frameworks (called MIL-101(Cr)@ CoO_x) and observed that these catalysts were active in transforming endogenous CO_2 to CO under ultrasonic irradiation (Fig. 7e).¹⁵⁰ The enhancement of CO supply inhibited cancer cell proliferation, resulting in a tumour regression rate of 86.4%, demonstrating the high efficiency of sonodynamic therapy. Despite this promising result, only few recent studies have utilised sonocatalysis to facilitate direct CO_2 activation. Islam *et al.* reported that Cu catalysts converted CO_2 to CO, CH_4 , C_2H_4 , HCOOH, and $\text{C}_2\text{H}_5\text{OH}$ under ultrasonication at 24 kHz, whereas these products were absent under silent

conditions.¹⁵⁵ Ma *et al.* investigated the sonocatalytic reduction of CO₂ using H₂Ti₃O₇ catalysts.¹⁵⁶ Applying ultrasound at 80 kHz resulted in the reduction of CO₂ to CO with 100% selectivity at a rate of 8.3 μmol g⁻¹ h⁻¹ using H₂Ti₃O₇ catalysts.¹⁵⁶ The high activity was caused by the synergy between the electronic properties of the catalyst and the sonoluminescence generated by the cavitation events. The H₂Ti₃O₇ catalysts also had good stability, with their activity remaining high after four consecutive cycles. The success of this approach is encouraging for future applications using sonocatalysis for CO₂ activation.

Finally, we introduce the perspective of using sonocatalysis in N₂ fixation. N₂ fixation (*i.e.*, activation of the N₂ molecule) is a very important application due to its crucial role in agriculture. Similar to CO₂ activation, the N≡N bond is extremely strong with a bond energy of 911 kJ mol⁻¹ that often requires the activation of a catalyst. Due to the high energy input required, N≡N bond activation occurs at elevated temperature (~500 °C) and pressure (~300 bar). These severe operating conditions make the process extremely energy intensive, thus contributing negatively to climate change. Several novel processes are being investigated to facilitate the activation of N₂ under ambient conditions, including electrocatalysis and plasma-catalysis. Sonocatalysis is also a promising approach to address this challenge. Recent works combining sonocatalysis and photocatalysis have demonstrated that this approach is feasible. Ding *et al.* synthesised N-TiO₂/Ti₃C₂ composite sonocatalysts and obtained good activity in converting N₂ to NH₃.¹⁵¹ The efficiency of sonocatalysis was further synergised with photocatalysis, achieving a NH₃ production rate of 415.6 μmol h⁻¹ g⁻¹ under ultrasonic irradiation at 53 kHz (Fig. 7f). Maimaitizi *et al.* also reported the effectiveness of flower-like Pt/N-MoS₂ microspheres in the sonocatalytic conversion of N₂.¹⁵⁷ Ranjith *et al.* prepared the hybrid structure by intercalating WS₂ into MXene Ti₃C₂T_x stacked with TiO₂ (called Ti₃C₂T_x/TiO₂-WS₂), which had an excellent charge transfer rate and high activity for sonophotocatalytic N₂ fixation.¹⁵⁸ The production rate of NH₃ from N₂ fixation on Ti₃C₂T_x/TiO₂-WS₂ reached 526 μmol g⁻¹ h⁻¹ at 40 kHz. These studies indicate that the development of sonocatalysts is a promising alternative for N₂ fixation.

4. Harnessing the power of microfluidics and materials nanostructuring in sonocatalysis

4.1. Current technical hurdles in sonocatalysis: energy efficiency and reaction control

Despite the promising synergy between heterogeneous catalysis and HFUS, the energy efficiency of current sonocatalytic processes is suboptimal. In sonochemical processes, the energy required to induce cavitation is supplied from electricity, which is converted by the piezoelectric transducer to generate ultrasound. Thus, electrical energy needs to be trans-

formed to mechanical energy before producing the ultrasonic irradiation. Moholkar *et al.* described the chain of energy conversion from electrical energy to the cavitation energy.¹⁵⁹ This process includes the transformation of electrical energy into mechanical oscillations of the piezoelectric crystal in the transducer. The kinetic energy of the vibration subsequently converts to the acoustic energy of ultrasound waves before finally transforming into cavitation energy, inducing physical and chemical effects upon bubble collapse. Rashwan *et al.* estimated that approximately 80–90% of electric energy could be transferred to the liquid *via* acoustic waves,¹³⁶ but that the proportion of acoustic waves that release cavitation energy is much smaller. The energy efficiency, η , is expressed by the ratio of the ultrasonic energy, Q_{US} , to the total supplied electric energy, Q_e , in the equation: $\eta = \frac{Q_{US}}{Q_e}$.¹⁶⁰

The term Q_{US} can be directly measured using calorimetry, and is determined from the rate of temperature increase during the ultrasonic irradiation using the equation:

$Q_{US} = C_p M \frac{dT}{dt}$, where C_p , M , and dT/dt are the heat capacity of the solvent, the mass of solvent, and the rate of temperature rise, respectively.^{160–162} This method is based on the assumption that mechanical energy in the transducer is fully converted to heat *via* cavitation and is solely responsible for the temperature change in the solution.¹⁶⁰ From the perspective of sonocatalysis, only the efficiency of the chemical effects resulting from cavitation events, *e.g.* the formation of ROS, is relevant. In some processes, only a small amount of total supplied energy is transformed into cavitation activity (<20%) to produce the desired chemical effects.^{163,164} Therefore, other criteria, including sonochemical efficiency (SE),^{165–167} cavitation yield^{168,169} and G-value,¹⁷⁰ are used for calibrating the efficiency of sonoreactors. The most popular criterion is the sonochemical efficiency, calculated as the number of \cdot OH radicals produced per unit of supplied energy *via* the equation:

$SE = \frac{n}{Q_e} = \frac{C \times V}{P \times t}$. In the previous equation, n , C , V , P , and t are the moles of \cdot OH radicals produced, molar concentration of OH radicals, sonoreactor, supplied ultrasonic power, and irradiation time, respectively. The concentration of \cdot OH radicals generated during ultrasonic irradiation can be detected using several methods, including potassium iodide (KI) dosimetry (Weissler method), ferrous sulphate dosimetry (Fricke dosimetry), terephthalic acid dosimetry, and TPPS dosimetry (monitoring the decomposition of porphyrin derivatives).^{162,171}

The sonochemical efficiency is influenced by many factors, including reactor design, applied ultrasonic frequency, power, temperature and choice of solvent.^{165,166,169,175–177} The three types of sonoreactors commonly reported in the literature are the emerged ultrasonic horn (Type-A), the bottom plate transducer/horn probe ultrasonic bath (Type-B) and the indirect ultrasonic bath (Type-C) (Fig. 8a).¹³⁶ Existing sonochemical techniques rely on the inception of cavitation bubbles in the liquid phase under the influence of an acoustic field to induce

The sonochemical efficiency is influenced by many factors, including reactor design, applied ultrasonic frequency, power, temperature and choice of solvent.^{165,166,169,175–177} The three types of sonoreactors commonly reported in the literature are the emerged ultrasonic horn (Type-A), the bottom plate transducer/horn probe ultrasonic bath (Type-B) and the indirect ultrasonic bath (Type-C) (Fig. 8a).¹³⁶ Existing sonochemical techniques rely on the inception of cavitation bubbles in the liquid phase under the influence of an acoustic field to induce

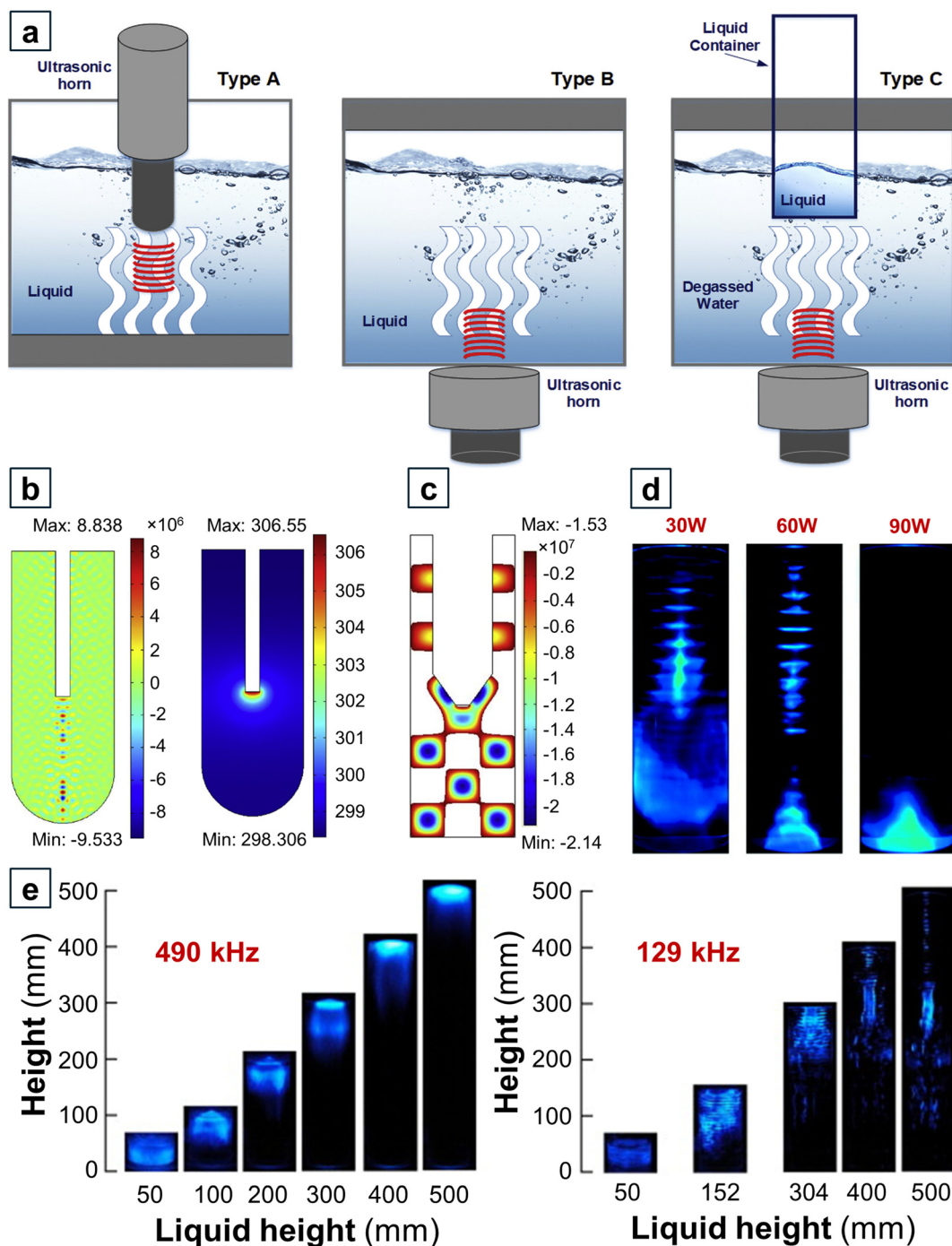


Fig. 8 (a) Three typical configurations of a sonoreactor, reproduced with permission from Rashwan *et al.*¹³⁶ Copyright 2019, Elsevier. (b) Pressure profile (left) and temperature contour (right) from cavitation bubble collapse under ultrasonic irradiation at 300 W, reproduced with permission from Rashwan *et al.*¹³⁶ Copyright 2019, Elsevier. (c) Active cavitation zones in a sonoreactor with oil–water phases, reproduced with permission from Niazi *et al.*¹⁷² Copyright 2014, Elsevier. (d) Sonochemical activity at different applied powers, expressed via chemiluminescence imaging, reproduced with permission from Son *et al.*¹⁷³ Copyright 2012, Elsevier. (e) Sonochemical luminescence at different ultrasonic frequencies and liquid heights of the cylindrical sonoreactor, reproduced with permission from Asakura *et al.*¹⁷⁴ Copyright 2008, Elsevier.

sonochemical effects. Kim *et al.* investigated cavitation bubble collapse under ultrasonic radiation at 300 W and showed that the pressure and temperature profiles were not homogeneously distributed within the entire volume of the reactor.¹⁷⁸

Even though pressure oscillations radiate perpendicularly away from the probe tip to the bottom of the reactor, hot spot regions were concentrated around the ultrasound probe (Fig. 8b).¹³⁶ Similarly, Niazi *et al.* simulated the ultrasonic acti-

vation of an aqueous solution saturated with oil at 25 °C in a glass cylindrical sonoreactor and obtained the formation of discrete active cavitation zones (Fig. 8c).¹⁷²

Due to the spatiotemporal unpredictability and stochastic nature of the bubble nucleation,¹⁸ extremely high ultrasonic intensities and prolonged continuous ultrasonic irradiation are often required to generate a sufficiently high density of inertial cavitation events in the fluid. The resulting rapid bubble implosion is essential for generating radicals, such as $\cdot\text{OH}$. However, these conditions lead to several undesirable side reactions and also induce unwanted secondary effects, such as high fluid shear stress and thermal effects.^{27,179} Furthermore, ultrasonic waves are quickly attenuated when propagating through the fluid at high ultrasonic intensities, resulting in the loss of acoustic energy to thermal energy as the liquid temperature increases during prolonged irradiation.¹⁸⁰ Son *et al.* examined the sonochemical activity in a reactor at different applied powers *via* chemiluminescence imaging with luminol.¹⁷³ The study found that the attenuation of ultrasound waves was stronger at higher applied ultrasound power. At a relatively high power (90 W), large cavitation bubbles were formed near the transducer.¹⁸¹ The highly concentrated cloud of bubbles hindered the transmission of ultrasonic waves, leading to their attenuation (Fig. 8d). The sonochemical efficiency also depends on the ultrasonic frequency. Asakura *et al.* visualised the sonochemical reaction field *via* chemiluminescence at different applied frequencies.¹⁷⁴ At higher ultrasonic frequencies, the intensity of sonochemical luminescence was stronger due to the production of more radicals. Sonochemical activity was even observed far away from the transducer (Fig. 8e). However, the energy consumption, materials cost, and material stability are major concerns at high frequency operation.¹⁸² At its current level, the sonochemical efficiency is still below its desired performance.^{167,183} Therefore, optimising the efficiency of sonocatalytic reactions by localising cavitation near the surface of the catalysts remains an important milestone in the field of sonocatalysis. The two most promising approaches for improving the energy efficiency of the sonochemical reactions are: (i) using nanostructured cavitation agents and (ii) optimising the design of sonoreactors. These two approaches are described in the subsequent sections.

Other challenges of sonocatalysis are the difficulty in exercising control over the reaction and in optimising the reactor performance. Due to the short lifespan of the active radicals generated from cavitation bubble collapse, very little mechanistic understanding has been gleaned for sonocatalytic reactions. The exact mechanism by which reactive radicals interact with the active sites of a catalyst remains largely unknown. This lack of knowledge represents a significant challenge for the optimization of sonocatalytic reactions and the design of highly active catalysts. Furthermore, due to the discrete distribution of active cavitation zones in the sonoreactor, effective mass and heat transfer within the entire reactor volume is sometimes difficult to achieve. This is especially true in the sonochemical synthesis of high value-added specialty chemi-

cals which require fine control over the reaction parameters. Optimisation of a sonoreactor is difficult since the overall sonochemical efficiency of a chemical process is influenced both by primary factors, such as frequency, intensity, and pressure, and secondary factors, like temperature and the choice of solvent. These complications lead to serious issues in the reproducibility of sonocatalytic research, hindering the development of its application. Finally, as most current sonoreactors are operated in batch-mode at laboratory-scale, scaling up the process poses an additional challenge. Significant time investments are necessary to perform the technical and economic evaluations of a sonocatalytic process, as well as the life cycle assessment of its sonoreactor. It is also important to evaluate the stability and durability of sonocatalysts to ensure a consistent performance and longer lifespan. Future investigation will likely focus on integrating sonocatalysis with renewable energy resources to make the technology more sustainable and more suitable for industrial-scale trials.

4.2. Designing catalytic cavitation agent to improve the energy efficiency of sonocatalysis

As described above, efficiently utilising ultrasonic energy for radical generation and chemical synthesis remains a key technical hurdle in the field of sonocatalysis. One method to overcome this problem is through the use of nanostructured cavitation agents that have engineered surface features to facilitate and localise cavitation. This method provides a convenient pathway to lower the acoustic energy consumption since the cavitation agent is able to compensate for the reduced energy input. In essence, cavitation events are confined near the active sites of these nanostructured materials, while no cavitation occurs in the bulk liquid. Indeed, spatial and temporal control of cavitation at specific ultrasonic frequencies and intensities is an issue that has already been addressed in biomedical acoustics, where HFUS cavitation is typically used for enhanced drug-delivery and ultrasound contrast enhancement.^{184–186} Importantly, the advances made in biomedical acoustics may have direct relevance in addressing the challenges in sonocatalysis using HFUS. Within the biomedical acoustics community, nanostructured cavitation agents are used to reduce the energy required for inertial cavitation by orders of magnitude.^{18,185,187–189} Thus, in a well-defined acoustic field, one could control the acoustic energy at a suitable level so that cavitation only occurs at the sites predefined by the cavitation agents.

Kwan *et al.* succeeded in designing polymeric nanocups that trapped and nucleated inertial cavitation bubbles on their surfaces (Fig. 9a).¹⁹⁰ High-speed imaging provided evidence that the implosion of the cavitation bubbles was occurring in close proximity of the cavitation agent, emphasising the effectiveness of this approach. Furthermore, the size of the nanocups could be easily tuned to make it suitable for various ultrasonic activation conditions. These nanocups improved the energy efficiency of sonochemical cavitation 30-fold. In other words, the inertial cavitation threshold is reduced from 30 MPa without the cavitation agents to only 1 MPa when the cavi-

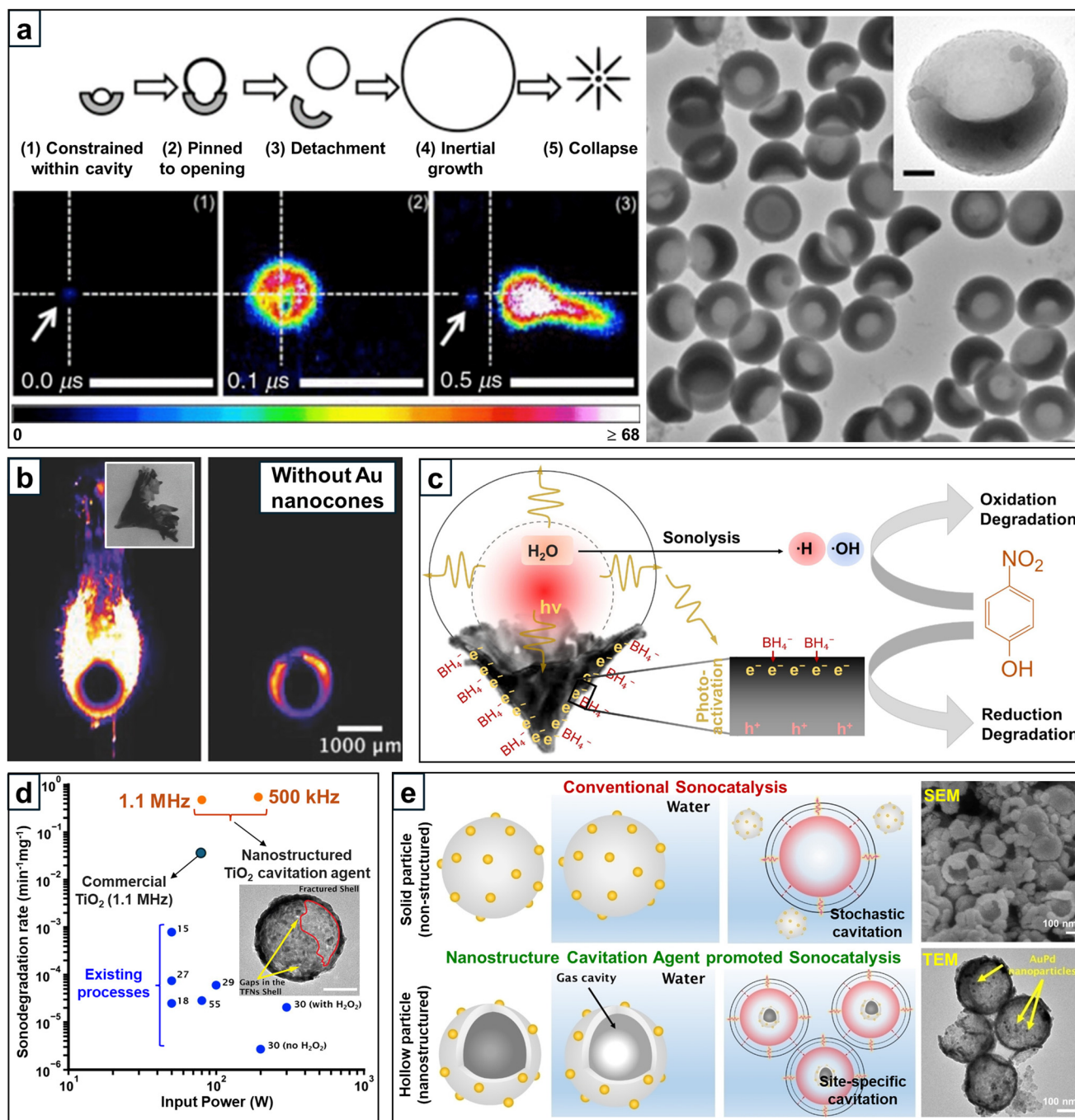


Fig. 9 (a) The use of polymeric nanocups as cavitation agents, showing stages (1), (2), and (3) of the cavitation nucleation mechanism, reproduced with permission from Kwan *et al.*¹⁹⁰ Copyright 2016, American Physical Society. (b) A cavitation event on a gold nanocone (left) and in the absence of a gold nanocone (right), reproduced with permission from Mannaris *et al.*¹⁸⁴ Copyright 2018, John Wiley and Sons. (c) Gas trapping and cavitation on a Au nanocone (Au NCs) resulting in the enhancement of its sonocatalytic activity, reproduced from an open access publication.¹⁹³ (d) Comparison of the sonochemical efficiency of nanostructured TiO_2 cavitation agents to other materials in the literature, reproduced from an open access publication.¹⁹⁴ (e) Enhanced energy efficiency and sonocatalytic activity of hollow AuPd/ TiO_2 nanoshells (AuPd/TON), reproduced with permission from Jonnalagadda *et al.*¹⁹⁵ Copyright 2022, John Wiley and Sons.

tation agents are included. Mannaris *et al.* prepared Au nanocones acting as cavitation agents and reported that their unique morphology was able to trap nanobubbles and facilitate inertial cavitation, greatly improving the sonochemical

efficiency (Fig. 9b).¹⁸⁴ Mesoporous silica have also been used as cavitation agents to enhance sonochemical efficiency.^{191,192}

However, despite the increased research into solid cavitation agents in biomedical engineering, there have been very

few reports using nanostructured cavitation agents to promote industrially relevant sonochemical reactions. Cavitation agents are usually engineered to have a large quantity of gas-stabilising sites, which are capable of nucleating, growing, and maintaining cavitation bubbles on their surface. However, in order to be used as a cavitation agent in sonocatalysis, the material also needs to be constructed from a catalytically active substance and/or possess a high density of active sites on its surface to facilitate chemical reactions. Therefore, to the nanoscale cavitation agents typically used in biomedical applications need to be redesigned to have dual functionality: as ultrasound-responsive cavitation agents and as heterogeneous catalysts.

Recently, progress has been made in this field with the introduction of the “catalytic cavitation agent”.^{193–196} Su *et al.* employed Au nanocones, which were established as effective cavitation agents, to catalyse the sono-degradation of water pollutants using 4-nitrophenol and methylene blue as model compounds (Fig. 9c).¹⁹³ The synergy between the ROS generated from cavitation events and the sonoluminescence-enhanced electron transfer resulting from the Au nanocones caused an 87-fold increase in the sonochemical degradation efficiency when compared to existing studies in literature. This demonstrates the vital role of localised cavitation events in sonocatalytic reactions. Jonnalagadda *et al.* synthesised TiO₂ fractured nanoshells that could serve as both effective cavitation nucleation agents and catalytically active sites.¹⁹⁴ The study showed that cavitation occurred locally on the TiO₂ fractured nanoshells, facilitating the *in situ* generation of active radicals that consequently degraded the organic pollutants (methylene blue) in the aqueous fluid, resulting in an enhancement of three orders of magnitude as compared to conventional methods (Fig. 9d). The sonocatalytic efficiency of TiO₂ fractured nanoshells was further improved after being decorated by AuPd nanoparticles that promoted both site-specific cavitation and high activity in the oxidation of benzyl alcohol to benzaldehyde (Fig. 9e). Jonnalagadda *et al.* reported that AuPd nanoparticles supported on TiO₂ fractured nanoshells (called AuPd/TONs) significantly reduced the energy requirement whilst achieving the same or even faster reaction rates when compared to the current advanced methods.¹⁹⁵ Most recently, Mahendran *et al.* engineered the CuO with multiple gas-stabilising sites (called CuO-MC) to act as both an effective cavitation nuclei and a highly active catalysts.¹⁹⁷ This material selectively facilitated the transfer of acoustic energy to the catalyst surface, minimise the loss of this energy into the bulk solution while remaining efficient cavitation properties at lower acoustic pressure amplitudes. Xie *et al.* utilised this synthesised CuO-MC and demonstrated that the selective sono-oxidation of glucose towards glucuronic acid could be achieved at minimised acoustic energy input.¹⁹⁸ These examples illustrate the great potential of synthesising cavitation agents using catalytically active materials to enable the direct utilization of radicals generated by cavitation for selective chemical reactions. The key point is that overall energy consumption of the process can be significantly reduced using these tailored nanostructured cavitation agents.

4.3. Harnessing the power of microfluidics in sonocatalysis

Reengineering the reactor is another approach to improving the energy efficiency of sonocatalytic processes. Existing sonochemistry techniques induce sonochemical effects by relying on inception cavitation in the liquid phase in poorly defined acoustic fields. In conventional sonochemistry setups (consisting of an ultrasonic bath, probe sonicator, and plate sonicator reaction chambers), predicting and controlling the occurrence of cavitation events is difficult due to the complex acoustic fields that arise from overlapping acoustic interferences. An appropriate reactor design with well-defined acoustic fields could achieve a means to control the frequency and location of inertial cavitation, significantly improving the energy efficiency. Wong *et al.* built a sono-reactor (called SonoCYL) with a cylindrically converging design that was capable of generating an intense and localised high acoustic pressure region (Fig. 10a).¹⁹⁹ This innovative sonochemical reactor had a much higher ·OH radical generation rate and energy efficiency than conventional reactors, demonstrating the crucial effect of reactor design on sonochemical activity.

Microfluidic reactors, also called microreactors are an important subset of sono-reactors. A microreactor is designed with channel sizes ranging from tens to hundreds of micrometers, allowing for fine control of chemical processes with a drastically reduced fluid volume. Whitesides has even stated that “microfluidics seems almost too good to be true: it offers so many advantages and so few disadvantages” in his Nature paper in 2006.²⁰⁰ The core advantages of microfluidics can overcome most challenges of conventional sonocatalytic reactions, such as controlling heat transfer, optimising discrete active zones, and scaling up batch-mode operation. Another benefit of microfluidic reactors is that they can handle reactions involving unstable or hazardous reactants. Microreactors in chemical processes using heterogeneous catalysts have been widely reported in Yao *et al.*,²⁰¹ Suryawanshi *et al.*,²⁰² Tanimu *et al.*²⁰³ and Feng *et al.*²⁰⁴ The combination of microfluidics and sonochemistry started to receive attention during the 2000s and early 2010s.^{205–211} Rivas *et al.* mentioned the term “micro-sono-reactor” as a green and efficient platform in his feature article in Chemical Communications in 2012,²¹² and later analysed the synergy of microfluidics and ultrasound as a process intensification concept in 2016.²¹³ One prominent advantage of microreactors for sonochemistry is their reproducibility, which is an issue that has often plagued conventional sono-reactors.

Recently, the combination of sonochemistry and ultrasound witnessed a surge of development thanks to the advances in acoustic engineering. With many new configurations possible for sono-micro-reactors, the energy efficiency has been significantly improved.^{101,214–217} The confined space within the microchannels allows for uniform distribution of active cavitation zones and generates well-defined acoustic fields and a means to control the frequency and location of inertial cavitation.^{218,219} Nieves *et al.* reported an enhancement of cavitation bubbles during the formation of mini-emulsions in

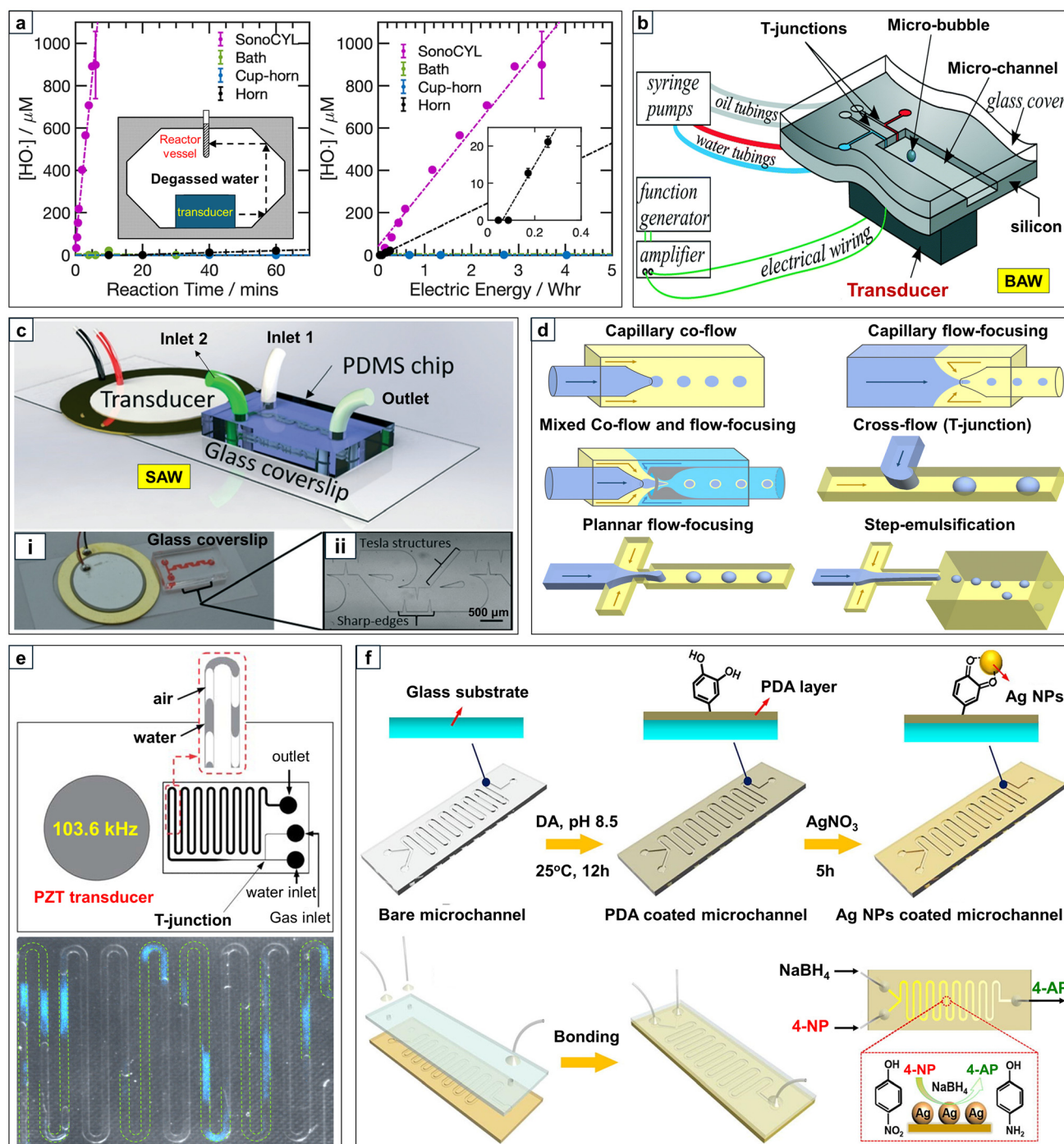


Fig. 10 (a) Sonochemical efficiency of the novel sonoreactor SonoCYL, reproduced from an open access publication.¹⁹⁹ (b) Setup of the microfluidic device with Bulk Acoustic Wave (BAW), reproduced from an open access publication.²³¹ (c) Surface Acoustic Wave (SAW) setup: (i) photo of the acoustofluidic device and (ii) a close-up of the microchannel design with sharp-edge structures and recirculation zones, reproduced with permission from Bachman *et al.*²³² Copyright 2020, Royal Society of Chemistry. (d) Different setups for generating droplets and microbubbles in a microreactor, reproduced with permission from Nan *et al.*²³⁷ Copyright 2024, Royal Society of Chemistry. (e) Schematic of a microfluidic T-junction device driven by an attached transducer (top) and chemiluminescence image of cavitation bubbles in the microchannel (bottom), reproduced with permission from Tandiono *et al.*²³⁸ Copyright 2010, Royal Society of Chemistry. (f) The process of immobilising Ag NPs on the wall of microchannels by polydopamine (PDA) coating and catalytic reduction of 4-NP to 4-AP in the microreactor, reproduced with permission from Zhang *et al.*²³⁹ Copyright 2017, Elsevier.

microchannels, resulting in the reduction of droplet polydispersity by 24%.²²⁰ Liu *et al.* also obtained a significant increase in the mixing efficiency when using the ultrasonic cavitation in microchannels.²²¹ Zhao *et al.* monitored cancer cell spheroids in a vascularised microfluidic model and found that microbubbles generated under ultrasonic irradiation in microchannels greatly enhanced the efficiency of cancer therapy.²²² Liu *et al.* obtained higher cavitation activity and better quality organic nanoparticles in a microfluidic device under ultrasonic irradiation at 20 kHz than when the same synthesis was performed *via* conventional methods.²²³ Zhao *et al.* observed an improved energy efficiency in the extraction of vanillin from water by an order of magnitude in a sonomicro-reactor.²²⁴ Thanks to the development of the interdigital transducer (IDT), extremely high frequency ultrasound (from several to hundreds of MHz) can now be generated in microfluidic devices. This research field has come to be known as “acoustofluidics” and has been extensively used in nanomaterials synthesis, material processing, and biomedical applications.^{225–230} However, the applications of acoustofluidics mainly relies on utilising the physical effects of sonochemistry, since the radical production at these extremely high ultrasonic frequencies is almost negligible (Fig. 3).

The combination of microfluidics and sonochemistry creates a platform that is highly effective and easily tuneable. Besides controlling the ultrasonic irradiation parameters (frequency and power), the flexibility of being able to use different transducer configurations and microchannel designs provide more degrees of freedom over which to optimise sonochemical reactions. The two main configurations of ultrasonic transducers inside a microreactor are Bulk Acoustic Wave (BAW) and Surface Acoustic Wave (SAW). In a BAW setup, the acoustic wave generated from the transducer is transferred to the bulk liquid and induces resonance modes in the microchannel (Fig. 10b).²³¹ In a SAW setup, the acoustic waves generated from the transducer or interdigitated transducer (IDTs) propagate along the surface of the substrate and radiate into the liquid along its path (Fig. 10c).²³² BAW microreactors are simpler, better characterised, and usually operate at a lower ultrasound frequency (tens kHz to 10 MHz) than SAW. SAW microreactors, on the other hand, require a more complicated fabrication process (patterning the transducer/IDT and bonding the microreactor on the substrate) but are often more precise, versatile, and flexible. More importantly, SAW microreactors are more energy efficient than BAW microreactors since the acoustic energy generated in SAW microreactors is confined to the surface of a substrate, whereas the acoustic energy generated in BAW microreactor is distributed throughout the bulk of substrate.²³³ Furthermore, the combination of multiple transducers/IDTs, even with different frequencies, can be used in SAW microreactors to generate different types of SAWs, such as the “travelling surface acoustic wave” (TSAW) and the “standing surface acoustic wave (SSAW)”.²³⁴ This capability allows for precise control of the generated acoustic wave, thus maximising the efficiency of manipulation processes, such as mixing, separation, concentration, sorting, trapping,

and patterning.^{235,236} These unique features make SAW microreactors a promising platform for the continued development of sonocatalysis.

In addition to the flexibility in setting up the configuration of the transducers/IDTs, the microchannels for fluid flow inside microreactors are amenable to numerous designs.^{234,240} To enhance cavitation during sonochemical processes, a higher density of microbubbles must be generated. Novel setups in gas/liquid mixing and microreactor geometries have been developed using microfluidics, allowing for the production of microbubbles with uniform size (Fig. 10d).²³⁷ Changing the identity of the gas and tuning the gas and liquid flow rates allow for more precise control over the density and compositions of microbubbles.²⁴¹ Microchannels can also be designed inside special structures to enhance the cavitation efficiency, as is the case in sharp-edge acoustofluidics.²⁴² Rasouli *et al.* constructed sharp-edge structures along the length of a microfluidic device and achieved superior performance in the synthesis of polymeric nanoparticles and liposome in a low-power and highly controllable process.²⁴³ Bachman *et al.* designed a SAW acoustofluidic device consisting of Tesla structures and periodic sharp-edge patterns, as depicted in Fig. 10c(i) and (ii).²³² This device exhibited a much higher mixing efficiency than conventional passive hydrodynamic mixers and was able to operate at a wide range of operating conditions. The subfields “micro-elastofluidics” and “stretchable microfluidics” were recently developed in Nguyen’s group at Griffith University. These microfluidics domains seek to manipulate the fluid-structure interactions of the sonomicroreactor^{244–247} to influence their sonochemical performance.

Despite recent reports of the enhanced energy efficiency of sono-microreactors, studies of the improved sonochemical efficiency of microfluidic devices are not as prevalent, despite their direct effect on sonocatalytic performance. In 2004, Iida *et al.* pioneered the quantification of $\cdot\text{OH}$ radical formation inside microreactors under the influence of ultrasound using fluorometry and obtained the first confirmation of cavitation events at the microscale. Tandiono *et al.* investigated the cavitation activity driven by capillary SAW in a microfluidic device made from PDMS and glass.²³⁸ The plate transducer was attached at a distance of 5 mm from the microreactor and produced ultrasonic waves at 103.6 kHz (Fig. 10e). High-speed images showed that strong inertial cavitation occurred at 136 μs and that most of the cavitation bubbles collapsed at 752 μs . Chemiluminescence experiments using luminol were carried out using the same setup, confirming the intensive formation of $\cdot\text{OH}$ radicals at the confined gas–liquid interfaces (Fig. 10e).²⁴⁸ This study provided direct evidence that cavitation bubbles do not occur randomly in the bulk liquid (as in conventional sonoreactors) but only within a well-defined region in the microreactor, allowing for the spatial control of sonochemical reactions. Rivas *et al.* designed a BAW microreactor engineered with cylindrical pits acting as gas trapping sites to nucleate cavitation and computed the sonochemical efficiency for the formation of $\cdot\text{OH}$ radicals from water sonoly-

sis occurring under different applied powers.^{211,249} They observed that the sonochemical efficiency was increased by an order of magnitude thanks to the presence of the designed pits, and that medium power delivered the highest performance in all cases. This study illustrates that the appropriate design of microchannel walls has the potential to intensify the formation of radical formations inside a sono-microreactor. Verhaagen *et al.* successfully scaled-up this pits-microreactor in 2016, increasing the sonochemical efficiency of the reactor by 45.1% and scaling up the capacity of the reactor by a factor of 25.¹⁶⁷ Thangavadeivel *et al.* evaluated the sonochemical efficiency of the 4-channels microreactor *via* the degradation of methyl orange.²⁵⁰ The formation of ROS from cavitation events was quantified by Fricke dosimetry and operational parameters including solution temperature, flow rate, and ultrasonic power were optimised to obtain the highest efficiency of the microreactor.

Heterogeneous catalysts need to be distributed homogeneously inside the microreactor in order to facilitate the reaction inside a microfluidic device as intended. Despite the challenge of mass transfer inside a narrow channel, several approaches have been developed to help accomplish this. The most popular approach is coating or immobilising solid catalysts on the wall of microchannels. Zhang *et al.* coated polydopamine (PDA) on the inside of a glass microchannel and used this PDA layer to anchor the Ag nanoparticles to the channel wall before bonding it with another glass cover to make the catalytic microreactor (Fig. 10f).²³⁹ Other approaches include loading the solid catalyst in a packed bed inside a microreactor or depositing catalysts *via* the functionalised monoliths in the microchannel.^{203,251} Recently, solid nanocatalysts were incorporated into the continuous phase of the microreactor, originally a mixture of liquid and gas, through the formation of Pickering emulsions, slurry Taylor segments, colloidal suspensions, and catalyst slurries. The homogeneous distribution of catalyst particles within the microfluidic channels helps to facilitate the reaction, enhancing the efficiency and overall conversion of microreactors.^{252–254} This approach is highly successful in leveraging the dual functionality of catalytic cavitation agents inside microfluidic devices in order to achieve the best efficiency for sonocatalytic reactions.

4.4. Density functional theory (DFT) calculations to assist in studying the mechanism of sonocatalytic reactions and designing catalytic cavitation agents for sonocatalysis

One challenge in the development of sonocatalysis is the lack of insights into the reaction mechanism. Without this crucial information, designing sonoreactors and sonocatalysts that maximise the production of desired products is reduced to a “trial-and-error” approach, which is costly and ineffective. Mechanistic insight into sonocatalytic reaction mechanisms by experimentation is very challenging due to the short life-span ROS and the large and inter-connected reaction network produced in ultrasonic irradiation. Computational studies *via* density functional theory (DFT) calculations provide a more tractable approach to gain a detailed understanding of sono-

chemical reactions at molecular level.^{255–258} Several DFT studies were reported recently that deliver novel insights into the reaction mechanism of the sonochemical transformation of biomass to high value-added specialty chemicals, significantly advancing the knowledge in this field and leading to the development of more efficient catalytic processes.

Glucose oxidation using heterogeneous catalysts usually results in the formation of gluconic acid as the main product.¹²³ Gluconic acid is used to make consumer products like household cleaners, industrial cleaners, inks, paints, dyes, and metal finishing, and its market price is AU\$92 per kg. However, it is also possible to produce glucuronic acid, a much more valuable chemical building block, from glucose oxidation. In fact, the market price of glucuronic acid is AU \$2.2M per kg because it is such a vital pharmaceutical intermediate in the production of drugs for blood coagulation inhibitors and antioxidants for immune system support. Glucuronic acid has been traditionally produced *via* enzymatic-catalysed routes and its production *via* heterogeneous catalysis was never effective enough to be commercially viable. However, in 2019, a successful strategy to produce glucuronic acid through the selective oxidation of glucose using a solid catalyst was developed by Amaniampong *et al.* as is shown in Fig. 11a.⁹⁸ Their work suggested that by using a CuO catalyst and tuning the reaction conditions, the glucose ring opening was inhibited and instead, selective oxidation at the C6 position was preferred, yielding glucuronic acid (Fig. 11a(i)).

DFT calculations showed that the ring opening of glucose was suppressed by the oxygen surface lattice of the CuO catalysts, which was able to trap the $\cdot\text{H}$ radicals produced by water sonolysis, as shown in Fig. 11a(ii).⁹⁸ DFT calculations predicted an activation barrier of 47 kJ mol⁻¹ for glucose ring opening on a clean CuO(111) surface, but that the barrier increases to 121 kJ mol⁻¹ under ultrasonic irradiation. Therefore, sonochemical conditions are a plausible alternative to controlling the opening of the glucose ring. Once glucose ring opening is suppressed, glucose in the closed-ring structure can be readily oxidised by $\cdot\text{OH}$ radicals, resulting in the highly selective production of glucuronic acid. The detailed reaction mechanism and computed activation barriers for all elementary steps are presented in Fig. 11a(iii). The presence of $\cdot\text{OH}$ radicals (from water sonolysis) on CuO(111) provides an alternative pathway with lower activation barriers (highlighted by blue arrows) for oxidising the glucose molecule. The mechanistic understanding reported herein is beneficial in thinking about how similar protocols can be implemented in modelling the conversion of other biomass resources *via* sonocatalysis.¹²²

Another challenge for sonocatalysis is that the active sites of the catalyst are not always well-defined, hindering the improvement and development of novel catalytic materials. In 2022, DFT calculations were applied to study the sonochemical conversion of cellulose to oxalic acid using Au/Fe₂O₃ catalysts.⁹⁹ The predicted adsorption energies and electronic properties calculated for different sites revealed that only the atoms located at narrow interfacial zones were active for cellulose oxidation (Fig. 11b(i)). DFT calculations showed that

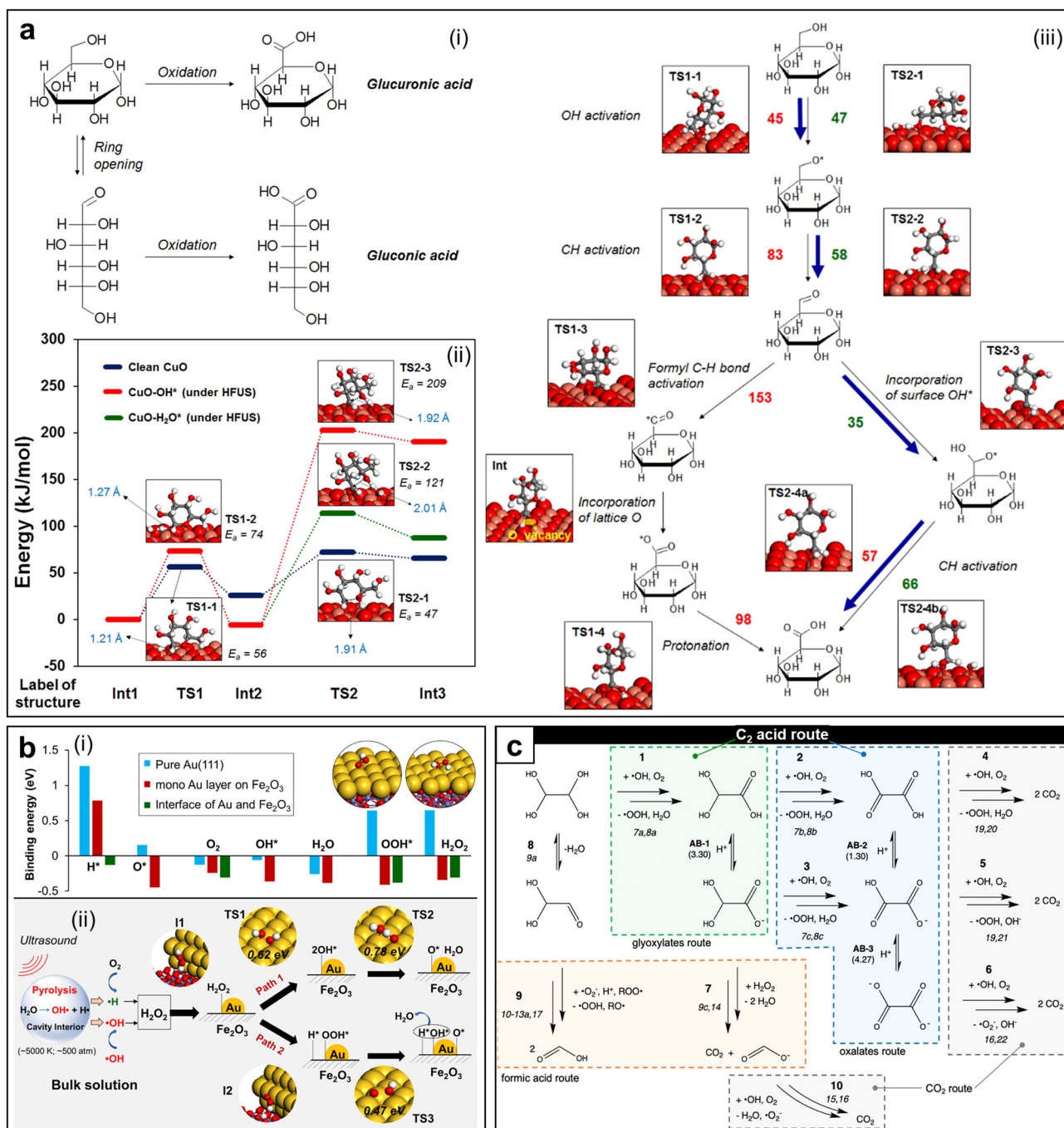


Fig. 11 (a) DFT investigation on the selective oxidation of glucose to glucuronic acid on CuO(111) surface under ultrasonic irradiation: (i) strategy to control the oxidation; (ii) inhibition of glucose ring opening under the activation of ultrasound; (iii) detailed mechanism of glucose oxidation to glucuronic acid with and without the ultrasound conditions, reproduced with permission from Amaniampong *et al.*⁹⁸ Copyright 2019, American Chemical Society. (b) Binding energies (i) and ROS formation mechanism (ii) at the interface of Au/Fe₂O₃ catalysts in ultrasonic activation conditions, reproduced with permission from Amaniampong *et al.*⁹⁹ Copyright 2022, Royal Society of Chemistry. (c) Reaction sono-oxidation network of glyoxal that yields C₂ acids, reproduced with permission from Fischer *et al.*²⁵⁹ Copyright 2024, John Wiley and Sons.

charge transfer between the Au nanoparticles and the Fe₂O₃ support induced a stronger stabilization of ROS at interfacial sites, facilitating the generation of oxidising agents ([•]OH, [•]OOH and [•]O) (Fig. 11b(ii)). This investigation established methodology for the rational development of sonocatalysts. It

particularly in the design of novel catalytic activation agents. This methodology was implemented in many studies using DFT calculations in order to design catalysts with higher activity and stability *via* doping and/or tuning the metal/support interactions.^{260–268}

Finally, DFT calculations also provide useful predictions of sonocatalytic efficiency. All kinetic and thermodynamic parameters for each elementary step in a sonochemical reaction can be computed and used as input data for validating a microkinetic model.^{259,269} Consequently, this yields estimates of rate constants and rate efficiencies under different reaction conditions. Fischer *et al.* performed extensive DFT calculations for all elementary steps pertaining to the oxidation of glyoxal of hydroxyl radicals and constructed a detailed microkinetic model (Fig. 11c).²⁵⁹ This model was used to evaluate the sonochemical efficiency of the reaction and optimised operating conditions, such as pH and the ultrasonic frequency, in order to obtain the desired product composition. All of their theoretical predictions were consistent with experimental measurements. It is expected that DFT calculations will become a key tool in accelerating the development of sonocatalysis and sustainable chemistry.

5. The contribution of sonochemistry and sonocatalysis to green chemistry

Following the official release of the “Twelve principles of Green Chemistry”,²⁷⁰ Cintas and Luche highlighted the contribution of sonochemical approaches to green chemistry in the field of chemical synthesis, materials science, and environmental science due to the use of less or non-toxic reagents or solvents under ambient conditions and their unique capabilities in controlling the selectivity and enhancing the rate of the reactions.²⁷¹ Indeed, sonochemistry is even called “distinctive chemistry”²⁷² and continuously considered nowadays as a green activation techniques in organics synthesis, as demonstrated clearly by Draye *et al.*^{273–275} and Machado *et al.*²⁷⁶ The

green context of sonochemistry has been recognised and discussed in details in environmental applications,¹⁷ food processing,²⁷⁷ and many other fields (polymer synthesis, nanomaterials, and pharmaceutical sciences...)²⁷⁸ The contribution of sonochemical approaches to green chemistry could be observed *via* the many principles, such as: (i) “Atom economy”: incorporating initial ingredients into the final product *via* mass transfer enhancement’ (ii) “Less hazardous chemical syntheses”: using a lower initiators and solvent inventory; (iii) “Safer solvents and auxiliaries”: using water as solvent; (iv) “Employing Renewable Feedstock”; (v) “Design for energy efficiency”, and (vi) “Inherently safer chemistry for accident prevention”.²⁷⁹ Fig. 12a illustrates the integration of sonochemistry into 12 design principles of Green Chemistry.

Besides contributing to green chemistry, sonochemistry also found applications in green engineering. According to the “12 principles of Green Engineering” which outline how to scale-up the production and make chemical processes greener,²⁸⁰ Mason *et al.* revealed the “green-link” between the physics, chemistry and engineering features of sonochemistry by analysing different industrial scale environmental processes.²⁸¹ The main advantages of sonochemistry are its potentially tuneable selectivity, enhancement of process efficiency, avoidance of toxic chemicals, reduction of waste, and consumption of renewable energy resources such as solar energy. Above features make sonochemistry a safe and energy-efficient discipline. Furthermore, Chatel *et al.* analysed the relationships between sonochemistry and green engineering focusing on different chemical processes and their energy efficiencies.²⁸² Sonochemistry also induced “green processes” in alimentary industry (filtrations, fermentations, sterilizations, emulsifications, extractions, dehydrations,...) due to its high-quality products, energy and solvent savings, lower mainten-

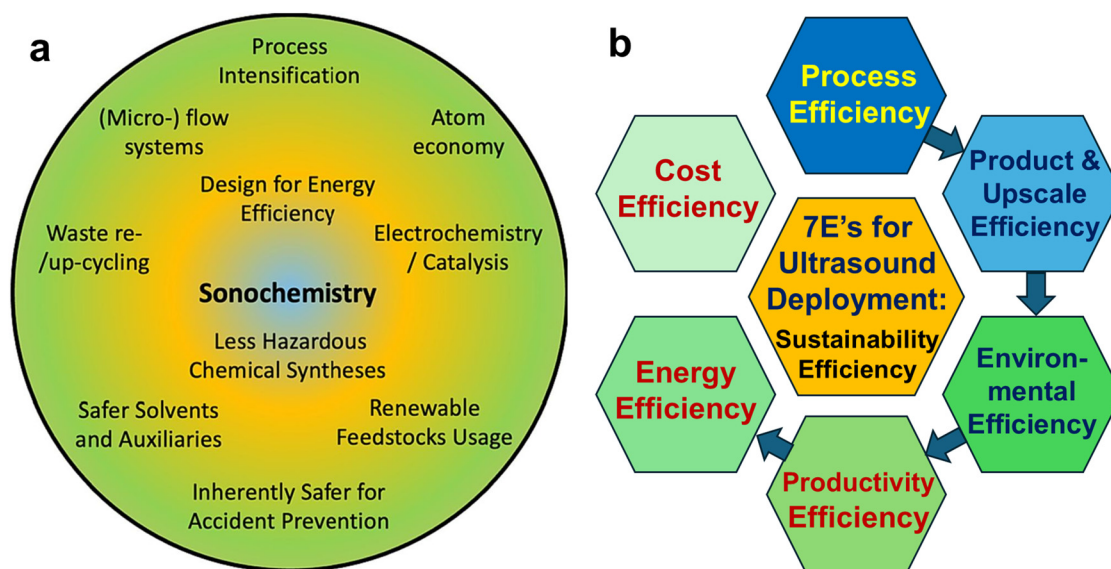


Fig. 12 (a) The integration between sonochemistry into 12 design principles of Green Chemistry, reproduced from an open access publication.²⁷⁹ (b) The concept of “7E” for evaluating ultrasonic efficiency in processing systems.

ance costs, shorter processing time and fewer wastes. Recently, Sivakumar *et al.* introduced the concept of “7E” to rationalise the seven different aspects of efficiency when analysing the implementation of sonochemistry in industries.²⁸³ The seven categories include efficiencies of process, product and scale-up, environment, productivity, energy, cost, and sustainability (Fig. 12b).

The combination of sonochemistry and a solid catalyst, called “sonocatalysis”, further leverage its relevance to green chemistry. Heterogeneous catalysis is a cornerstone of green chemistry,²⁷⁶ owing to its unique features such as: utilising a small amount of materials for significant enhancement of process efficiency, controllable selectivity of the reaction, reduction of waste and increasing atom economy. Chatel also mentioned that if the experimental parameters could be optimised, the majority of sonocatalytic reactions would be in favour of almost all principles of green chemistry and often greener than those carried out without the application of ultrasound.²⁸⁴ Benefiting from the distinctive synergy effects, sonocatalysis has a great potential in converting various renewable feedstocks to high-value specialty chemicals which are generally inaccessible by conventional catalytic routes.¹⁰¹ Sonocatalysis facilitates the production of those specialty chemicals with unprecedented high selectivity and efficiency, promoting principles of green chemistry such as “atom economy” and “reduce derivatives”.

Finally, the combination of sonocatalysis and microfluidics, as analysed in section 4, represents an additional innovative perspective in term of green chemistry. The greenness of microfluidics was clearly emphasised by its capabilities in handling small quantities of reagents and solvents and therefore reducing the waste, precisely controlling reaction conditions, facilitating faster and safer protocols. A debate exists in literature about the compatibility between green chemistry and sonochemistry for reactions involving hazardous compounds.^{284–286} However, this problem can be easily overcome with microfluidic solutions. The application of microfluidics in sonocatalysis also enhances the spatial control of sonochemical reactions, confining the reactions closely to the interface of gas–liquid, leading to better yield and higher atom economy.

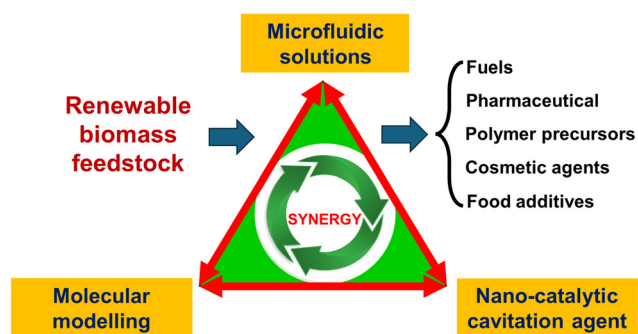


Fig. 13 The synergy between microfluidics, catalytic cavitation agents, and molecular modelling in the sustainable transformation of renewable biomass to high value-added products.

6. Conclusions and perspectives

This review provides a comprehensive picture of the current status and future perspectives of sonocatalysis, an important subsection of sonochemistry. Sonochemistry is now widely considered to be a vital green technology. Much progress has been made in tuning the selectivity of products, minimising the use of harmful chemicals or reagents, reducing waste, and shifting to renewable energy resources. Sonochemistry is highly effective in cleaning and extraction applications, environmental remediation, organic synthesis, biomedical treatment, and nanomaterial synthesis.

Sonocatalysis is based on the synergy between heterogeneous catalysis and ultrasound in order to facilitate chemical reactions. The core of this approach relies on generating highly reactive radicals *via* rapid cavitation under high frequency ultrasonic irradiation in the presence of a solid catalyst. Recent advances in wastewater treatment and sonotherapy *via* sonocatalysis were presented in this manuscript. In addition, the sonocatalytic mechanism was analysed, highlighting the synergy between solid catalysts and ultrasound, and giving insight into the design of more efficient sonochemical processes. This manuscript also focuses on the applications of sonocatalysis in biomass conversion, which is a promising approach for addressing climate change and promoting the development of a circular economy through sustainable chemistry. The introduction of renewable biomass resources in the chemical industry promotes the sustainable production of environmentally friendly chemicals and a wide range of products essential for human life (Fig. 13). The application of sonocatalysis in biomass conversion allows for fine-tuning of the product distribution in order to transform biomass-derived feedstocks into high value-added specialty chemicals and access to chemicals that are generally impossible to produce by conventional routes. This research reviewed was compiled with the intention of analysing the current state of sonocatalysis, as well as highlighting the potential for further development in the future.

The major technical hurdles of sonocatalysis in its current state are the low efficiency in utilising ultrasonic energy for radical generation, and the difficulties in reaction control. These challenges have been reviewed and analysed in detail. Several promising approaches to overcoming these problems have been identified, including the use of catalytic cavitation agents and the design of microfluidic sonoreactors. Using tailored nanostructured catalytic cavitation agents causes a significant reduction in the energy consumption of sonocatalytic processes. Implementing catalytic cavitation agents in a microfluidic sonoreactor with a well-defined acoustic field allows for fine control over the acoustic energy so that cavitation only occurs at the site of the nanostructured cavitation agents. In this way, the majority of radicals produced inside the cavitation bubble are transferred directly to a nano-engineered catalytic surface, enhancing the activity and selectivity of the reaction. The application of molecular modelling *via* density functional theory (DFT) calculations results in fundamental insight

into the sonocatalytic reaction mechanism at the atomic scale. Microkinetic models supported by DFT calculations and validated by experimental measurements guide the design of novel bifunctional nanomaterials that serve as both effective cavitation agents and active catalysts. The integration of nanostructured catalytic cavitation agents, microfluidic solutions, and molecular modelling forms a trilateral methodology that allows researchers to unlock the full potential of sonocatalysis for sustainably chemistry.

Data availability

No primary research results, software or code has been included and no new data were generated or analysed as part of this review.

Conflicts of interest

The authors declare no conflict of interest.

Acknowledgements

This work is financially supported by the Australian Research Council (FL230100023 and DE240100408). Y. C. acknowledges financial support from the Zhejiang University Luk's Scholarship for Graduates International Exchange for the cooperation research conducted at Griffith University. P. N. A. acknowledges the financial support from the European Research Council (ERC) funded/Co-funded by the European Union (ERC, ConCASM, project agreement number 101117070). Views and opinions expressed are however those of the author(s) only and do not necessarily reflect those of the European Union or the European Research Council. Neither the European Union nor the granting authority can be held responsible for them. F. J. and P. N. A. also acknowledge financial support from the European Union (ERDF) and Région Nouvelle Aquitaine.

References

- N. H. Ince, G. Tezcanli, R. K. Belen and İ. G. Apikyan, *Appl. Catal., B*, 2001, **29**, 167–176.
- S. K. Gujar, G. Divyapriya, P. R. Gogate and P. V. Nidheesh, *Crit. Rev. Environ. Sci. Technol.*, 2023, **53**, 780–802.
- T. D. Pham, R. A. Shrestha, J. Virkutyte and M. Sillanpää, *Can. J. Civ. Eng.*, 2009, **36**, 1849–1858.
- J. Li, Y. Ma, T. Zhang, K. K. Shung and B. Zhu, *BME Front.*, 2022, **2022**, 9764501.
- H. Huang, Y. Zheng, M. Chang, J. Song, L. Xia, C. Wu, W. Jia, H. Ren, W. Feng and Y. Chen, *Chem. Rev.*, 2024, **124**, 8307–8472.
- H.-V. Tran, T. T. Dang, N. H. Nguyen, H. T. Tran, D. T. Nguyen, D. V. Do, T. S. Le, T. H. Ngo, Y. K. E. Late, P. N. Amaniampong, E. Fletcher, T. Q. Hung, Y. Cheng, T.-K. Nguyen, T. S. Tran, J. Zhang, H. An, N.-T. Nguyen and Q. T. Trinh, *ChemSusChem*, 2025, **18**, e202401974.
- C. Xiouras, A. Fytopoulos, J. Jordens, A. G. Boudouvis, T. Van Gerven and G. D. Stefanidis, *Ultrason. Sonochem.*, 2018, **43**, 184–192.
- P. W. Cains, P. D. Martin and C. J. Price, *Org. Process Res. Dev.*, 1998, **2**, 34–48.
- H. Li, H. Li, Z. Guo and Y. Liu, *Ultrason. Sonochem.*, 2006, **13**, 359–363.
- J. Ferreira, J. Opsteyn, F. Rocha, F. Castro and S. Kuhn, *Chem. Eng. Res. Des.*, 2020, **162**, 249–257.
- R. Crespo, P. M. Martins, L. Gales, F. Rocha and A. M. Damas, *J. Appl. Crystallogr.*, 2010, **43**, 1419–1425.
- Z. J. Dolatowski, J. Stadnik and D. Stasiak, *Acta Sci. Pol., Technol. Aliment.*, 2007, **6**, 88–99.
- T. S. Awad, H. A. Moharram, O. E. Shaltout, D. Asker and M. M. Youssef, *Food Res. Int.*, 2012, **48**, 410–427.
- M. Gallo, L. Ferrara and D. Naviglio, *Foods*, 2018, **7**, 164.
- W. Zhang, Y. Shi, S. Abd Shukor, A. Vijayakumaran, S. Vlatakis, M. Wright and M. Thanou, *Nanoscale*, 2022, **14**, 2943–2965.
- A. L. Y. Kee and B. M. Teo, *Ultrason. Sonochem.*, 2019, **56**, 37–45.
- B. Savun-Hekimoğlu, *Acoustics*, 2020, **2**, 766–775.
- R. G. Thomas, U. S. Jonnalagadda and J. J. Kwan, *Langmuir*, 2019, **35**, 10106–10115.
- Y. T. Shah, A. B. Pandit and V. S. Moholkar, in *Cavitation Reaction Engineering*, Springer US, Boston, MA, 1999, pp. 155–192.
- M. Mrowetz, C. Pirola and E. Selli, *Ultrason. Sonochem.*, 2003, **10**, 247–254.
- Z. Li, L. Li, S. Zhang, L. Zhang, Y. Cui and H. Shi, *Sep. Purif. Technol.*, 2024, **332**, 125799.
- D. Meroni, M. Jiménez-Salcedo, E. Falletta, B. M. Bresolin, C. F. Kait, D. C. Boffito, C. L. Bianchi and C. Pirola, *Ultrason. Sonochem.*, 2020, **67**, 105123.
- S. A. Asli and M. Taghizadeh, *ChemistrySelect*, 2020, **5**, 13720–13731.
- D. Meroni, C. Gasparini, A. Di Michele, S. Ardizzone and C. L. Bianchi, *Ultrason. Sonochem.*, 2020, **66**, 105119.
- A. Qayyum, D. A. Giannakoudakis, D. Łomot, R. F. Colmenares-Quintero, K. Nikiforow, A. P. LaGrow and J. C. Colmenares, *Ultrason. Sonochem.*, 2024, **104**, 106829.
- B. H. Hosseini, R. L. Oliveira, D. Łomot, O. Chernyayeva and J. C. Colmenares Quintero, *Molecules*, 2024, **29**, 1436.
- T. G. McKenzie, F. Karimi, M. Ashokkumar and G. G. Qiao, *Chem. – Eur. J.*, 2019, **25**, 5372–5388.
- P. N. Amaniampong, A. Karam, Q. T. Trinh, K. Xu, H. Hirao, F. Jérôme and G. Chatel, *Sci. Rep.*, 2017, **7**, 40650.
- K. S. Suslick, N. C. Eddingsaas, D. J. Flannigan, S. D. Hopkins and H. Xu, *Acc. Chem. Res.*, 2018, **51**, 2169–2178.

- 30 I. Tzanakis, G. S. B. Lebon, D. G. Eskin and K. A. Pericleous, *Ultrason. Sonochem.*, 2017, **34**, 651–662.
- 31 H. Xu, B. W. Zeiger and K. S. Suslick, *Chem. Soc. Rev.*, 2013, **42**, 2555–2567.
- 32 M. Ashokkumar, *ChemTexts*, 2018, **4**, 7.
- 33 S. Manickam, D. C. Boffito, E. M. M. Flores, J.-M. Leveque, R. Pflieger, B. G. Pollet and M. Ashokkumar, *Ultrason. Sonochem.*, 2023, **99**, 106540.
- 34 D. J. Flannigan and K. S. Suslick, *Nature*, 2005, **434**, 52–55.
- 35 M. M. Hasan and K. S. Iyengar, *Nature*, 1963, **199**, 995–996.
- 36 A. Brotchie, F. Grieser and M. Ashokkumar, *Phys. Rev. Lett.*, 2009, **102**, 084302.
- 37 K. S. Suslick, S. J. Doktycz and E. B. Flint, *Ultrasonics*, 1990, **28**, 280–290.
- 38 K. S. Suslick, *Science*, 1990, **247**, 1439–1445.
- 39 K. Feng, J. Eshraghi, P. P. Vlachos and H. Gomez, *Phys. Fluids*, 2024, **36**, 053305.
- 40 Y. Yang, M. Shan, Y. Zhang, H. Li, X. Kan and Q. Han, *Comput. Fluids*, 2024, **279**, 106325.
- 41 G. Chatel, L. Novikova and S. Petit, *Appl. Clay Sci.*, 2016, **119**, 193–201.
- 42 R. F. Martínez, G. Cravotto and P. Cintas, *J. Org. Chem.*, 2021, **86**, 13833–13856.
- 43 K. S. Suslick, P. F. Schubert and J. W. Goodale, *J. Am. Chem. Soc.*, 1981, **103**, 7342–7344.
- 44 N. H. Tran, L. Hoang, L. D. Nghiem, N. M. H. Nguyen, H. H. Ngo, W. Guo, Q. T. Trinh, N. H. Mai, H. Chen, D. D. Nguyen, T. T. Ta and K. Y.-H. Gin, *Sci. Total Environ.*, 2019, **692**, 157–174.
- 45 Y. Zhao, D. Liu, W. Huang, Y. Yang, M. Ji, L. D. Nghiem, Q. T. Trinh and N. H. Tran, *Bioresour. Technol.*, 2019, **288**, 121619.
- 46 N. H. Tran, Q. T. Trinh and Q. B. Nguyen, *Sci. Total Environ.*, 2019, **685**, 1308–1309.
- 47 P. Qiu, B. Park, J. Choi, B. Thokchom, A. B. Pandit and J. Khim, *Ultrason. Sonochem.*, 2018, **45**, 29–49.
- 48 Q. T. Trinh, T. Le Van, T. T. N. Phan, K. P. Ong, H. Kosslick, P. N. Amaniampong, M. B. Sullivan, H.-S. Chu, H. An, T.-K. Nguyen, J. Zhang, J. Zhang, P. T. Huyen and N.-T. Nguyen, *J. Alloys Compd.*, 2024, **1002**, 175322.
- 49 P. Aryal, C. Hefner, B. Martinez and C. S. Henry, *Lab Chip*, 2024, **24**, 1175–1206.
- 50 Y. Zhang, J. Li, S. Jiao, Y. Li, Y. Zhou, X. Zhang, B. Maryam and X. Liu, *Sci. Total Environ.*, 2024, **929**, 172734.
- 51 M. Yew, Y. Ren, K. S. Koh, C. Sun and C. Snape, *Global Challenges*, 2019, **3**, 1800060.
- 52 G. Wang and H. Cheng, *Molecules*, 2023, **28**, 3706.
- 53 S. Soni, A. Kumari, S. Sharma, A. Sharma, V. Sheel, R. Thakur, S. K. Bhatia and A. K. Sharma, *J. Taiwan Inst. Chem. Eng.*, 2025, **166**, 105565.
- 54 P. Liu, Z. Wu, A. V. Abramova and G. Cravotto, *Ultrason. Sonochem.*, 2021, **74**, 105566.
- 55 J. Abdi, A. J. Sisi, M. Hadipoor and A. Khataee, *J. Hazard. Mater.*, 2022, **424**, 127558.
- 56 P. Dhull, A. Sudhaik, P. Raizada, S. Thakur, V.-H. Nguyen, Q. Van Le, N. Kumar, A. A. Parwaz Khan, H. M. Marwani, R. Selvasembian and P. Singh, *Chemosphere*, 2023, **333**, 138873.
- 57 B.-M. Jun, J. Han, C. M. Park and Y. Yoon, *Ultrason. Sonochem.*, 2020, **64**, 104993.
- 58 M. Dastborhan, A. Khataee, S. Arefi-Oskoui and Y. Yoon, *Ultrason. Sonochem.*, 2022, **87**, 106058.
- 59 K. Saravanakumar, A. Fayyaz, S. Park, Y. Yoon, Y. M. Kim and C. M. Park, *J. Mol. Liq.*, 2021, **344**, 117740.
- 60 J. Qiao, M. Lv, Z. Qu, M. Zhang, X. Cui, D. Wang, C. Piao, Z. Liu, J. Wang and Y. Song, *Sci. Total Environ.*, 2019, **689**, 178–192.
- 61 K. Shanmugam Ranjith, S. Majid Ghoreishian, S. Han, N. R. Chodankar, G. Seeta Rama Raju, S. J. Marje, Y. S. Huh and Y.-K. Han, *Ultrason. Sonochem.*, 2023, **99**, 106570.
- 62 Á. d. J. Ruiz-Baltazar, *Ultrason. Sonochem.*, 2021, **73**, 105521.
- 63 A. Ucar, *Russ. J. Appl. Chem.*, 2022, **95**, 1364–1372.
- 64 S. S. Magdum, M. Bhosale, G. Palanisamy, K. Selvakumar, S. Thangarasu and T. H. Oh, *J. Water Process Eng.*, 2024, **59**, 104997.
- 65 M. Sadeghi, S. Farhadi and A. Zabardasti, *New J. Chem.*, 2020, **44**, 20878–20894.
- 66 A. Jamal Sisi, A. Khataee, M. Fathinia, B. Vahid and Y. Orooji, *J. Mol. Liq.*, 2020, **316**, 113801.
- 67 Y. Vasseghian, E.-N. Dragoi, F. Almomani and V. T. Le, *Chemosphere*, 2022, **287**, 132387.
- 68 G. Li, Y. Cao, L. Yi, J. Wang and Y. Song, *J. Chem. Technol. Biotechnol.*, 2020, **95**, 1756–1772.
- 69 G. Wang and H. Cheng, *Sci. Total Environ.*, 2023, **901**, 165833.
- 70 J. Qiao, H. Zhang, G. Li, S. Li, Z. Qu, M. Zhang, J. Wang and Y. Song, *Sep. Purif. Technol.*, 2019, **211**, 843–856.
- 71 G. Wang, S. Li, X. Ma, J. Qiao, G. Li, H. Zhang, J. Wang and Y. Song, *Ultrason. Sonochem.*, 2018, **45**, 150–166.
- 72 M. F. Dadjour, C. Ogino, S. Matsumura and N. Shimizu, *Biochem. Eng. J.*, 2005, **25**, 243–248.
- 73 M. Farshbaf Dadjour, C. Ogino, S. Matsumura, S. Nakamura and N. Shimizu, *Water Res.*, 2006, **40**, 1137–1142.
- 74 C. Ogino, M. Farshbaf Dadjour, K. Takaki and N. Shimizu, *Biochem. Eng. J.*, 2006, **32**, 100–105.
- 75 S. Haddadi, A. Khataee, S. Arefi-Oskoui, B. Vahid, Y. Orooji and Y. Yoon, *Ultrason. Sonochem.*, 2023, **92**, 106255.
- 76 Q. Liu, L. Shi, Y. Liao, X. Cao, X. Liu, Y. Yu, Z. Wang, X. Lu and J. Wang, *Adv. Sci.*, 2022, **9**, 2200005.
- 77 Z. Feng, X. Xiang, J. Huang, L. Wang, B. Zhu, H. Zhou, H. Pang, C. Cheng, L. Ma and L. Qiu, *Adv. Funct. Mater.*, 2023, **33**, 2302579.
- 78 S. Son, J. H. Kim, X. Wang, C. Zhang, S. A. Yoon, J. Shin, A. Sharma, M. H. Lee, L. Cheng, J. Wu and J. S. Kim, *Chem. Soc. Rev.*, 2020, **49**, 3244–3261.

- 79 F. Yang, J. Lv, W. Ma, Y. Yang, X. Hu and Z. Yang, *Small*, 2024, **20**, 2402669.
- 80 S. Liu, K. Dou, B. Liu, M. Pang, P. a. Ma and J. Lin, *Angew. Chem., Int. Ed.*, 2023, **62**, e202301831.
- 81 G. Chen, J. Du, L. Gu, Q. Wang, Q. Qi, X. Li, R. Zhang, H. Yang, Y. Miao and Y. Li, *Chem. Eng. J.*, 2024, **482**, 148953.
- 82 J. Yagi, A. Ikeda, L.-C. Wang, C.-S. Yeh and H. Kawasaki, *J. Phys. Chem. C*, 2022, **126**, 19693–19704.
- 83 M. Chang, L. Zhang, Z. Wang, L. Chen, Y. Dong, J. Yang and Y. Chen, *Adv. Drug Delivery Rev.*, 2024, **205**, 115160.
- 84 J. Fouladi, A. AlNouss and T. Al-Ansari, *J. Cleaner Prod.*, 2023, **418**, 138071.
- 85 J. G. Segovia-Hernández, G. Contreras-Zarazúa and C. Ramírez-Márquez, *RSC Sustainability*, 2023, **1**, 1332–1353.
- 86 Q. T. Trinh, A. Banerjee, K. B. Ansari, D. Q. Dao, A. Drif, N. T. Binh, D. T. Tung, P. M. Q. Binh, P. N. Amaniampong, P. T. Huyen and M. T. Le, in *Biorefinery of Alternative Resources: Targeting Green Fuels and Platform Chemicals*, ed. S. Nanda, D.-V. N. Vo and P. K. Sarangi, Springer Singapore, Singapore, 2020, pp. 317–353.
- 87 P. N. Amaniampong, N. Y. Asiedu, E. Fletcher, D. Doodoo-Arhin, O. J. Olatunji and Q. T. Trinh, in *Valorization of Biomass to Value-Added Commodities: Current Trends, Challenges, and Future Prospects*, ed. M. O. Daramola and A. O. Ayeni, Springer International Publishing, Cham, 2020, pp. 193–220.
- 88 K. B. Ansari, S. Z. Hassan, S. A. Farooqui, R. Hasib, P. Khan, A. R. S. Rahman, M. S. Khan and Q. T. Trinh, in *Green Diesel: An Alternative to Biodiesel and Petrodiesel*, ed. M. Aslam, S. Shivaji Maktedar and A. K. Sarma, Springer Nature Singapore, Singapore, 2022, pp. 351–375.
- 89 R. Paul, C. Sarkar, Y. Yan, Q. T. Trinh, B. S. Rao, C.-W. Pao, J.-F. Lee, W. Liu and J. Mondal, *ChemCatChem*, 2020, **12**, 3687–3704.
- 90 C. Sarkar, S. C. Shit, D. Q. Dao, J. Lee, N. H. Tran, R. Singuru, K. An, D. N. Nguyen, Q. V. Le, P. N. Amaniampong, A. Drif, F. Jerome, P. T. Huyen, T. T. N. Phan, D.-V. N. Vo, N. Thanh Binh, Q. T. Trinh, M. P. Sherburne and J. Mondal, *Green Chem.*, 2020, **22**, 2049–2068.
- 91 M. T. Le, V. H. Do, D. D. Truong, E. Bruneel, I. Van Driessche, A. Riisager, R. Fehrmann and Q. T. Trinh, *Ind. Eng. Chem. Res.*, 2016, **55**, 4846–4855.
- 92 K. B. Ansari, A. Banerjee, M. Danish, S. Z. Hassan, D. V. Sahayaraj, M. S. Khan, T. T. N. Phan and Q. T. Trinh, in *Innovations in Thermochemical Technologies for Biofuel Processing*, ed. S. Nanda and D.-V. Vo, Elsevier, 2022, pp. 115–147.
- 93 K. B. Ansari, M. Danish, A. Banerjee, S. Z. Hassan, D. V. Sahayaraj, M. S. Khan, P. T. Huyen and Q. T. Trinh, in *Innovations in Thermochemical Technologies for Biofuel Processing*, ed. S. Nanda and D.-V. Vo, Elsevier, 2022, pp. 21–62.
- 94 D. B. Nguyen, S. Saud, Q. T. Trinh, H. An, N.-T. Nguyen, Q. H. Trinh, H. T. Do, Y. S. Mok and W. G. Lee, *Plasma Chem. Plasma Process.*, 2023, **43**, 1475–1488.
- 95 R. Paul, R. Das, N. Das, S. Chakraborty, C.-W. Pao, Q. Thang Trinh, G. T. K. Kalhara Gunasooriya, J. Mondal and S. C. Peter, *Angew. Chem., Int. Ed.*, 2023, **62**, e202311304.
- 96 G. Liu, P. R. Narangari, Q. T. Trinh, W. Tu, M. Kraft, H. H. Tan, C. Jagadish, T. S. Choksi, J. W. Ager, S. Karuturi and R. Xu, *ACS Catal.*, 2021, **11**, 11416–11428.
- 97 A. Denra, S. Saud, D. B. Nguyen, Q. T. Trinh, T.-K. Nguyen, H. An, N.-T. Nguyen, S. Teke and Y. S. Mok, *J. Cleaner Prod.*, 2024, **436**, 140618.
- 98 P. N. Amaniampong, Q. T. Trinh, K. De Oliveira Vigier, D. Q. Dao, N. H. Tran, Y. Wang, M. P. Sherburne and F. Jérôme, *J. Am. Chem. Soc.*, 2019, **141**, 14772–14779.
- 99 P. N. Amaniampong, Q. T. Trinh, T. Bahry, J. Zhang and F. Jérôme, *Green Chem.*, 2022, **24**, 4800–4811.
- 100 M. Paquin, É. Loranger, V. Hannaux, B. Chabot and C. Daneault, *Ultrason. Sonochem.*, 2013, **20**, 103–108.
- 101 P. N. Amaniampong and F. Jérôme, *Curr. Opin. Green Sustainable Chem.*, 2020, **22**, 7–12.
- 102 P. N. Amaniampong, J.-L. Clément, D. Gignes, C. Ortiz Mellet, J. M. García Fernández, Y. Blériot, G. Chatel, K. De Oliveira Vigier and F. Jérôme, *ChemSusChem*, 2018, **11**, 2673–2676.
- 103 A. Hernoux-Villière, U. Lassi and J.-M. Lévêque, *Ultrason. Sonochem.*, 2013, **20**, 1341–1344.
- 104 M. Kunaver, E. Jasiukaityté and N. Čuk, *Bioresour. Technol.*, 2012, **103**, 360–366.
- 105 M. Montalbo-Lomboy, L. Johnson, S. K. Khanal, J. van Leeuwen and D. Grewell, *Bioresour. Technol.*, 2010, **101**, 351–358.
- 106 S. Tallarico, P. Costanzo, S. Bonacci, A. Macario, M. L. Di Gioia, M. Nardi, A. Procopio and M. Oliverio, *Sci. Rep.*, 2019, **9**, 18858.
- 107 D. Rinsant, G. Chatel and F. Jérôme, *ChemCatChem*, 2014, **6**, 3355–3359.
- 108 F. Napoly, N. Kardos, L. Jean-Gérard, C. Goux-Henry, B. Andrioletti and M. Draye, *Ind. Eng. Chem. Res.*, 2015, **54**, 6046–6051.
- 109 A. Sarwono, Z. Man, N. Muhammad, A. S. Khan, W. S. W. Hamzah, A. H. A. Rahim, Z. Ullah and C. D. Wilfred, *Ultrason. Sonochem.*, 2017, **37**, 310–319.
- 110 S. Marullo, C. Rizzo, A. Meli and F. D'Anna, *ACS Sustainable Chem. Eng.*, 2019, **7**, 5818–5826.
- 111 R. Behling, G. Chatel and S. Valange, *Ultrason. Sonochem.*, 2017, **36**, 27–35.
- 112 S. Haouache, A. Karam, T. Chave, J. Clarhaut, P. N. Amaniampong, J. M. Garcia Fernandez, K. De Oliveira Vigier, I. Capron and F. Jérôme, *Chem. Sci.*, 2020, **11**, 2664–2669.
- 113 B. Liu, B. Du, Y. Sun, M. Zhu, Y. Yang, X. Wang and J. Zhou, *Fuel Process. Technol.*, 2020, **203**, 106387.
- 114 Z. M. A. Bundhoo and R. Mohee, *Ultrason. Sonochem.*, 2018, **40**, 298–313.

- 115 M. J. Bussemaker, F. Xu and D. Zhang, *Bioresour. Technol.*, 2013, **148**, 15–23.
- 116 Q. T. Trinh, B. K. Chethana and S. H. Mushrif, *J. Phys. Chem. C*, 2015, **119**, 17137–17145.
- 117 B. Du, C. Chen, Y. Sun, M. Yu, M. Yang, X. Wang and J. Zhou, *Fuel Process. Technol.*, 2020, **206**, 106479.
- 118 B. Du, B. Liu, X. Wang and J. Zhou, *ChemistryOpen*, 2019, **8**, 643–649.
- 119 B. Du, B. Liu, Y. Yang, X. Wang and J. Zhou, *Catalysts*, 2019, **9**, 399.
- 120 P. Bujak, P. Bartzczak and J. Polanski, *J. Catal.*, 2012, **295**, 15–21.
- 121 B. Toukoniitty, J. Kuusisto, J.-P. Mikkola, T. Salmi and D. Y. Murzin, *Ind. Eng. Chem. Res.*, 2005, **44**, 9370–9375.
- 122 T. Bahry, S. Jiang, U. Jonnalagadda, W. Liu, B. Teychene, F. Jerome, S. H. Mushrif and P. N. Amaniampong, *Catal. Sci. Technol.*, 2023, **13**, 2982–2993.
- 123 P. N. Amaniampong, Q. T. Trinh, B. Wang, A. Borgna, Y. Yang and S. H. Mushrif, *Angew. Chem., Int. Ed.*, 2015, **54**, 8928–8933.
- 124 P. N. Amaniampong, Q. T. Trinh, K. Li, S. H. Mushrif, Y. Hao and Y. Yang, *Catal. Today*, 2018, **306**, 172–182.
- 125 P. N. Amaniampong, Q. T. Trinh, J. J. Varghese, R. Behling, S. Valange, S. H. Mushrif and F. Jérôme, *Green Chem.*, 2018, **20**, 2730–2741.
- 126 K. B. Ansari, A. Banerjee, S. Z. Hassan, M. Danish, I. Arman, P. Khan, A. R. Shakeelur Rahman, Q. N. Ahmad and Q. T. Trinh, in *2D Nanomaterials for CO₂ Conversion into Chemicals and Fuels*, ed. K. K. Sadasivuni, K. Kannan, A. M. Abdullah and B. Kumar, The Royal Society of Chemistry, 2022, pp. 270–300.
- 127 O. Mohan, Q. T. Trinh, A. Banerjee and S. H. Mushrif, *Mol. Simul.*, 2019, **45**, 1163–1172.
- 128 Q. Hassan, S. Algburi, A. Z. Sameen, M. Jaszczur and H. M. Salman, *Environ. Syst. Decis.*, 2024, **44**, 327–350.
- 129 Q. T. Trinh, J. Yang, J. Y. Lee and M. Saeys, *J. Catal.*, 2012, **291**, 26–35.
- 130 R. Li, Z. Liu, Q. T. Trinh, Z. Miao, S. Chen, K. Qian, R. J. Wong, S. Xi, Y. Yan, A. Borgna, S. Liang, T. Wei, Y. Dai, P. Wang, Y. Tang, X. Yan, T. S. Choksi and W. Liu, *Adv. Mater.*, 2021, **33**, 2101536.
- 131 M. A. Tekalgne, K. V. Nguyen, D. L. T. Nguyen, V.-H. Nguyen, T. P. Nguyen, D.-V. N. Vo, Q. T. Trinh, A. Hasani, H. H. Do, T. H. Lee, H. W. Jang, H. S. Le, Q. V. Le and S. Y. Kim, *J. Alloys Compd.*, 2020, **823**, 153897.
- 132 T. T. Dang, T. L. A. Nguyen, K. B. Ansari, V. H. Nguyen, N. T. Binh, T. T. N. Phan, T. H. Pham, D. T. T. Hang, P. N. Amaniampong, E. Kwao-Boateng and Q. T. Trinh, in *Nanostructured Photocatalysts*, ed. V.-H. Nguyen, D.-V. N. Vo and S. Nanda, Elsevier, 2021, pp. 169–216.
- 133 P. J. Buchanan, Z. Chase, R. J. Matear, S. J. Phipps and N. L. Bindoff, *Nat. Commun.*, 2019, **10**, 4611.
- 134 N. Ojha, K. K. Pant and E. Coy, *Ind. Eng. Chem. Res.*, 2023, **62**, 21885–21908.
- 135 S. S. Rashwan, I. Dincer and A. Mohany, *Int. J. Energy Res.*, 2019, **43**, 1045–1048.
- 136 S. S. Rashwan, I. Dincer, A. Mohany and B. G. Pollet, *Int. J. Hydrogen Energy*, 2019, **44**, 14500–14526.
- 137 M. H. Islam, O. S. Burheim and B. G. Pollet, *Ultrason. Sonochem.*, 2019, **51**, 533–555.
- 138 S. Merouani, O. Hamdaoui, Y. Rezgui and M. Guemini, *Int. J. Hydrogen Energy*, 2016, **41**, 832–844.
- 139 S. Merouani, O. Hamdaoui, Y. Rezgui and M. Guemini, *Ultrason. Sonochem.*, 2015, **22**, 41–50.
- 140 S. S. Rashwan, I. Dincer and A. Mohany, *Int. J. Hydrogen Energy*, 2020, **45**, 20808–20819.
- 141 L. Venault, "Reactivity of the Uranium (U(IV)/U(VI)) and the Plutonium (Pu(m)/Pu(TV)) in nitric aqueous solution under Ultrasound", PhD thesis, Université de Paris-Sud, 1997..
- 142 M. Yuan, S. Liang, L. Yang, F. Li, B. Liu, C. Yang, Z. Yang, Y. Bian, P. a. Ma, Z. Cheng and J. Lin, *Adv. Mater.*, 2023, **35**, 2209589.
- 143 J. Shi, *Natl. Sci. Rev.*, 2023, **10**, nwad101.
- 144 C. Xia, A. Wu, Z. Jin, L. Zeng, L. Jiang, Q. Xu, M. Fan and Q. He, *Biomaterials*, 2023, **296**, 122090.
- 145 Y. Wang, D. Zhao, H. Ji, G. Liu, C. Chen, W. Ma, H. Zhu and J. Zhao, *J. Phys. Chem. C*, 2010, **114**, 17728–17733.
- 146 W. Qi, J. Liu, X. Guo, H. Guo, T. Thomas, Y. Zhu, S. Liu and M. Yang, *ACS Appl. Nano Mater.*, 2023, **6**, 2636–2645.
- 147 B. G. Pollet, F. Foroughi, A. Y. Faid, D. R. Emberson and M. H. Islam, *Ultrason. Sonochem.*, 2020, **69**, 105238.
- 148 F. Foroughi, C. I. Bernäcker, L. Röntzsch and B. G. Pollet, *Ultrason. Sonochem.*, 2022, **84**, 105979.
- 149 Y. Zhang, H. Khanbareh, S. Dunn, C. R. Bowen, H. Gong, N. P. H. Duy and P. T. T. Phuong, *Adv. Sci.*, 2022, **9**, 2105248.
- 150 T. Zhang, Q. Zheng, J. Huang and X. Li, *Adv. Funct. Mater.*, 2024, **34**, 2311029.
- 151 Z. Ding, M. Sun, W. Liu, W. Sun, X. Meng and Y. Zheng, *Sep. Purif. Technol.*, 2021, **276**, 119287.
- 152 G. Glockler, *J. Phys. Chem.*, 1958, **62**, 1049–1054.
- 153 M. H. Islam, O. S. Burheim, J.-Y. Hihn and B. G. Pollet, *Ultrason. Sonochem.*, 2021, **73**, 105474.
- 154 M. Yuan, L. Yang, Z. Yang, Z. Ma, J. Ma, Z. Liu, P. a. Ma, Z. Cheng, A. Maleki and J. Lin, *Adv. Sci.*, 2024, **11**, 2308546.
- 155 M. H. Islam, H. Mehrabi, R. H. Coridan, O. S. Burheim, J.-Y. Hihn and B. G. Pollet, *Ultrason. Sonochem.*, 2021, **72**, 105401.
- 156 J. Ma, X. Xiong, C. Ban, K. Wang, J.-Y. Dai and X. Zhou, *Appl. Phys. Lett.*, 2022, **121**, 263901.
- 157 H. Maimaitizi, A. Abulizi, T. Zhang, K. Okitsu and J.-j. Zhu, *Ultrason. Sonochem.*, 2020, **63**, 104956.
- 158 K. S. Ranjith, S. M. Ghoreishian, R. Umaphathi, G. S. R. Raju, H. U. Lee, Y. S. Huh and Y.-K. Han, *Ultrason. Sonochem.*, 2023, **100**, 106623.
- 159 V. S. Moholkar and M. M. C. G. Warmoeskerken, *AIChE J.*, 2003, **49**, 2918–2932.
- 160 M. Toma, S. Fukutomi, Y. Asakura and S. Koda, *Ultrason. Sonochem.*, 2011, **18**, 197–208.
- 161 J.-j. Zhou, H.-m. Peng and J.-h. Hu, in 2011 Symposium on Piezoelectricity, Acoustic Waves and Device Applications (SPAWDA), 2011, pp. 48–51.

- 162 S. Koda, T. Kimura, T. Kondo and H. Mitome, *Ultrason. Sonochem.*, 2003, **10**, 149–156.
- 163 N. P. Vichare, P. Senthilkumar, V. S. Moholkar, P. R. Gogate and A. B. Pandit, *Ind. Eng. Chem. Res.*, 2000, **39**, 1480–1486.
- 164 J.-M. Löning, C. Horst and U. Hoffmann, *Ultrason. Sonochem.*, 2002, **9**, 169–179.
- 165 J. A. Kewalramani, B. Bezerra de Souza, R. W. Marsh and J. N. Meegoda, *Ultrason. Sonochem.*, 2023, **98**, 106529.
- 166 Y. Asakura and K. Yasuda, *Ultrason. Sonochem.*, 2021, **81**, 105858.
- 167 B. Verhaagen, Y. Liu, A. G. Pérez, E. Castro-Hernandez and D. Fernandez Rivas, *ChemistrySelect*, 2016, **1**, 136–139.
- 168 R. Feng, Y. Zhao, C. Zhu and T. J. Mason, *Ultrason. Sonochem.*, 2002, **9**, 231–236.
- 169 S. Asgharzadehahmadi, A. A. Abdul Raman, R. Parthasarathy and B. Sajjadi, *Renewable Sustainable Energy Rev.*, 2016, **63**, 302–314.
- 170 Y. T. Didenko and K. S. Suslick, *Nature*, 2002, **418**, 394–397.
- 171 D. B. Rajamma, S. Anandan, N. S. M. Yusof, B. G. Pollet and M. Ashokkumar, *Ultrason. Sonochem.*, 2021, **72**, 105413.
- 172 S. Niazi, S. H. Hashemabadi and M. M. Razi, *Chem. Eng. Res. Des.*, 2014, **92**, 166–173.
- 173 Y. Son, M. Lim, J. Khim and M. Ashokkumar, *Ultrason. Sonochem.*, 2012, **19**, 16–21.
- 174 Y. Asakura, T. Nishida, T. Matsuoka and S. Koda, *Ultrason. Sonochem.*, 2008, **15**, 244–250.
- 175 M. W. A. Kuijpers, M. F. Kemmere and J. T. F. Keurentjes, *Ultrasonics*, 2002, **40**, 675–678.
- 176 I. Garcia-Vargas, O. Louisnard and L. Barthe, *Ultrason. Sonochem.*, 2023, **99**, 106542.
- 177 K. Yasuda, T. T. Nguyen and Y. Asakura, *Ultrason. Sonochem.*, 2018, **43**, 23–28.
- 178 K. Y. Kim, K.-T. Byun and H.-Y. Kwak, *Chem. Eng. J.*, 2007, **132**, 125–135.
- 179 J. Collins, T. G. McKenzie, M. D. Nothling, M. Ashokkumar and G. G. Qiao, *Polym. Chem.*, 2018, **9**, 2562–2568.
- 180 M. A. Beckett and I. Hua, *J. Phys. Chem. A*, 2001, **105**, 3796–3802.
- 181 S. Merouani and O. Hamdaoui, *Ultrason. Sonochem.*, 2016, **32**, 320–327.
- 182 J. Chen, C. Fei, D. Lin, P. Gao, J. Zhang, Y. Quan, D. Chen, D. Li and Y. Yang, *Front. Mater.*, 2022, **8**, 733358.
- 183 M. Singla and N. Sit, in *Energy Aspects of Acoustic Cavitation and Sonochemistry*, ed. O. Hamdaoui and K. Kerboua, Elsevier, 2022, pp. 349–373.
- 184 C. Mannaris, B. M. Teo, A. Seth, L. Bau, C. Coussios and E. Stride, *Adv. Healthcare Mater.*, 2018, **7**, 1800184.
- 185 Z. Gao, W. Wu and B. Wang, *J. Fluid Mech.*, 2021, **911**, A20.
- 186 R. Myers, C. Coviello, P. Erbs, J. Foloppe, C. Rowe, J. Kwan, C. Crake, S. Finn, E. Jackson, J.-M. Balloul, C. Story, C. Coussios and R. Carlisle, *Mol. Ther.*, 2016, **24**, 1627–1633.
- 187 A. Sazgarnia, A. Shanei, A. R. Taheri, N. T. Meibodi, H. Eshghi, N. Attaran and M. M. Shanei, *J. Ultrasound Med.*, 2013, **32**, 475–483.
- 188 A. Yildirim, R. Chattaraj, N. T. Blum and A. P. Goodwin, *Chem. Mater.*, 2016, **28**, 5962–5972.
- 189 J. J. Kwan, R. Myers, C. M. Coviello, S. M. Graham, A. R. Shah, E. Stride, R. C. Carlisle and C. C. Coussios, *Small*, 2015, **11**, 5305–5314.
- 190 J. J. Kwan, G. Lajoinie, N. de Jong, E. Stride, M. Versluis and C. C. Coussios, *Phys. Rev. Appl.*, 2016, **6**, 044004.
- 191 Y. Zhao, Y. Zhu, J. Fu and L. Wang, *Chem. – Asian J.*, 2014, **9**, 790–796.
- 192 Q. Feng, W. Zhang, X. Yang, Y. Li, Y. Hao, H. Zhang, L. Hou and Z. Zhang, *Adv. Healthcare Mater.*, 2018, **7**, 1700957.
- 193 X. Su, U. S. Jonnalagadda, L. D. Bharatula and J. J. Kwan, *Ultrason. Sonochem.*, 2021, **79**, 105753.
- 194 U. S. Jonnalagadda, X. Su and J. J. Kwan, *Ultrason. Sonochem.*, 2021, **73**, 105530.
- 195 U. S. Jonnalagadda, Q. Fan, X. Su, W. Liu and J. J. Kwan, *ChemCatChem*, 2022, **14**, e202200732.
- 196 Z. Zong, E. Gilbert, C. C. Y. Wong, L. Usadi, Y. Qin, Y. Huang, J. Raymond, N. Hankins and J. Kwan, *Ultrason. Sonochem.*, 2023, **101**, 106669.
- 197 V. Mahendran, Q. T. Trinh, X. Zhangyue, U. Jonnalagadda, T. Gould, N.-T. Nguyen, J. Kwan, T. S. Choksi, W. Liu, S. Valange, F. Jérôme and P. N. Amaniampong, *Angew. Chem.*, 2025, **64**, e202416543.
- 198 Z. Xie, V. Mahendran, U. S. Jonnalagadda, Q. Fan, X. Su, A. F. Fischer, M. Tan, L. Tao, F. Jérôme, J. J. Kwan, S. Valange, T. S. Choksi, P. N. Amaniampong and W. Liu, *Green Chem.*, 2025, **27**, 573–585.
- 199 C. C. Y. Wong, J. L. Raymond, L. N. Usadi, Z. Zong, S. C. Walton, A. C. Sedgwick and J. Kwan, *Ultrason. Sonochem.*, 2023, **99**, 106559.
- 200 G. M. Whitesides, *Nature*, 2006, **442**, 368–373.
- 201 X. Yao, Y. Zhang, L. Du, J. Liu and J. Yao, *Renewable Sustainable Energy Rev.*, 2015, **47**, 519–539.
- 202 P. L. Suryawanshi, S. P. Gumfekar, B. A. Bhanvase, S. H. Sonawane and M. S. Pimplapure, *Chem. Eng. Sci.*, 2018, **189**, 431–448.
- 203 A. Tanimu, S. Jaenicke and K. Alhooshani, *Chem. Eng. J.*, 2017, **327**, 792–821.
- 204 H. Feng, Y. Zhang, J. Liu and D. Liu, *Molecules*, 2022, **27**, 8052.
- 205 J. Jordens, A. Honings, J. Degève, L. Braeken and T. V. Gerven, *Ultrason. Sonochem.*, 2013, **20**, 1345–1352.
- 206 L. Johansson, J. Enlund, S. Johansson, I. Katardjiev and V. Yantchev, *Biomed. Microdevices*, 2012, **14**, 279–289.
- 207 J. Friend and L. Y. Yeo, *Rev. Mod. Phys.*, 2011, **83**, 647–704.
- 208 Y. Iida, K. Yasui, T. Tuziuti, M. Sivakumar and Y. Endo, *Chem. Commun.*, 2004, 2280–2281.
- 209 Y. Iida, T. Tuziuti, K. Yasui, A. Towata and T. Kozuka, *Ultrason. Sonochem.*, 2007, **14**, 621–626.

- 210 S. Hübner, S. Kressirer, D. Kralisch, C. Bludszuweit-Philipp, K. Lukow, I. Jänich, A. Schilling, H. Hieronymus, C. Liebner and K. Jähnisch, *ChemSusChem*, 2012, **5**, 279–288.
- 211 D. Fernandez Rivas, A. Prosperetti, A. G. Zijlstra, D. Lohse and H. J. G. E. Gardeniers, *Angew. Chem., Int. Ed.*, 2010, **49**, 9699–9701.
- 212 D. Fernandez Rivas, P. Cintas and H. J. G. E. Gardeniers, *Chem. Commun.*, 2012, **48**, 10935–10947.
- 213 D. Fernandez Rivas and S. Kuhn, *Top. Curr. Chem.*, 2016, **374**, 70.
- 214 P. Mohanty, R. Mahapatra, P. Padhi, C. V. V. Ramana and D. K. Mishra, *Nano-Struct. Nano-Objects*, 2020, **23**, 100475.
- 215 B. Richard, C. Shahana, R. Vivek, A. Reddy M and P. A. Rasheed, *Nanoscale*, 2023, **15**, 18156–18172.
- 216 K. Yiannacou and V. Sariola, *Langmuir*, 2021, **37**, 4192–4199.
- 217 W. Kim, B. Cha, J. S. Jeon and J. Park, *Sens. Actuators, B*, 2023, **393**, 134132.
- 218 A. Rosales Pérez and K. Esquivel Escalante, *ChemPlusChem*, 2024, **89**, e202300660.
- 219 Y. Bian, F. Guo, S. Yang, Z. Mao, H. Bachman, S.-Y. Tang, L. Ren, B. Zhang, J. Gong, X. Guo and T. J. Huang, *Microfluid. Nanofluid.*, 2017, **21**, 132.
- 220 E. Nieves, G. Vite, A. Kozina and L. F. Olguin, *Ultrason. Sonochem.*, 2021, **74**, 105556.
- 221 Y. Liu, J. Ran, S. Yin, S. Li, W. Huang and L. Zhang, *Chem. Eng. Process. – Process Intensif.*, 2023, **194**, 109573.
- 222 P. Zhao, Y. Peng, Y. Wang, Y. Hu, J. Qin, D. Li, K. Yan and Z. Fan, *Ultrason. Sonochem.*, 2023, **101**, 106709.
- 223 Z. Liu, M. Yang, W. Yao, T. Wang and G. Chen, *Chem. Eng. Sci.*, 2023, **280**, 119052.
- 224 S. Zhao, C. Yao, L. Liu and G. Chen, *Chem. Eng. J.*, 2022, **450**, 138185.
- 225 H. Wang, F. Yuan, Z. Xie, C. Sun, F. Wu, R. Mikhaylov, M. Shen, J. Yang, Y. Zhou, D. Liang, X. Sun, Z. Wu, Z. Yang and X. Yang, *Appl. Acoust.*, 2023, **205**, 109258.
- 226 D. Huang, J. Wang, J. Che, B. Wen and W. Kong, *Biomed. Technol.*, 2023, **1**, 1–9.
- 227 Y. Fan, X. Wang, J. Ren, F. Lin and J. Wu, *Microsyst. Nanoeng.*, 2022, **8**, 94.
- 228 J. M. Rothberg, T. S. Ralston, A. G. Rothberg, J. Martin, J. S. Zahorian, S. A. Alie, N. J. Sanchez, K. Chen, C. Chen, K. Thiele, D. Grosjean, J. Yang, L. Bao, R. Schneider, S. Schaetz, C. Meyer, A. Neben, B. Ryan, J. R. Petrus, J. Lutsky, D. McMahill, G. Corteville, M. R. Hageman, L. Miller and K. G. Fife, *Proc. Natl. Acad. Sci. U. S. A.*, 2021, **118**, e2019339118.
- 229 N. Ota, Y. Yalikul, T. Suzuki, S. W. Lee, Y. Hosokawa, K. Goda and Y. Tanaka, *R. Soc. Open Sci.*, 2019, **6**, 181776.
- 230 Y. Li, S. Cai, H. Shen, Y. Chen, Z. Ge and W. Yang, *Biomicrofluidics*, 2022, **16**, 031502.
- 231 I. Leibacher, P. Reichert and J. Dual, *Lab Chip*, 2015, **15**, 2896–2905.
- 232 H. Bachman, C. Chen, J. Rufo, S. Zhao, S. Yang, Z. Tian, N. Nama, P.-H. Huang and T. J. Huang, *Lab Chip*, 2020, **20**, 1238–1248.
- 233 X. Ding, P. Li, S.-C. S. Lin, Z. S. Stratton, N. Nama, F. Guo, D. Slotcavage, X. Mao, J. Shi, F. Costanzo and T. J. Huang, *Lab Chip*, 2013, **13**, 3626–3649.
- 234 Z. Chen, Z. Pei, X. Zhao, J. Zhang, J. Wei and N. Hao, *Chem. Eng. J.*, 2022, **433**, 133258.
- 235 X. Zhao, Z. Chen, Y. Qiu and N. Hao, *Mater. Adv.*, 2023, **4**, 988–994.
- 236 P. Zhang, H. Bachman, A. Ozcelik and T. J. Huang, *Annu. Rev. Anal. Chem.*, 2020, **13**, 17–43.
- 237 L. Nan, H. Zhang, D. A. Weitz and H. C. Shum, *Lab Chip*, 2024, **24**, 1135–1153.
- 238 T. Tandiono, S.-W. Ohl, D. S.-W. Ow, E. Klaseboer, V. V. T. Wong, A. Camattari and C.-D. Ohl, *Lab Chip*, 2010, **10**, 1848–1855.
- 239 L. Zhang, Z. Liu, Y. Wang, R. Xie, X.-J. Ju, W. Wang, L.-G. Lin and L.-Y. Chu, *Chem. Eng. J.*, 2017, **309**, 691–699.
- 240 A. Mudugamuwa, U. Roshan, S. Hettiarachchi, H. Cha, H. Musharaf, X. Kang, Q. T. Trinh, H. M. Xia, N.-T. Nguyen and J. Zhang, *Small*, 2024, **20**, 2404685.
- 241 H. Lin, J. Chen and C. Chen, *Med. Biol. Eng. Comput.*, 2016, **54**, 1317–1330.
- 242 Z. Chen, P. Liu, X. Zhao, L. Huang, Y. Xiao, Y. Zhang, J. Zhang and N. Hao, *Appl. Mater. Today*, 2021, **25**, 101239.
- 243 M. R. Rasouli and M. Tabrizian, *Lab Chip*, 2019, **19**, 3316–3325.
- 244 H. Fallahi, H. Cha, H. Adelnia, Y. Dai, H. T. Ta, S. Yadav, J. Zhang and N.-T. Nguyen, *Nanoscale Horiz.*, 2022, **7**, 414–424.
- 245 H. M. Musharaf, U. Roshan, A. Mudugamuwa, Q. T. Trinh, J. Zhang and N.-T. Nguyen, *Micromachines*, 2024, **15**, 897.
- 246 D. T. Tran, A. S. Yadav, N.-K. Nguyen, P. Singha, C. H. Ooi and N.-T. Nguyen, *Small*, 2023, **20**, 2303435.
- 247 H. H. Vu, N.-T. Nguyen, N.-K. Nguyen, C. H. Luu, S. Hettiarachchi and N. Kashaninejad, *Adv. Eng. Mater.*, 2023, **25**, 2300821.
- 248 S.-W. Ohl, D. S. W. Ow, E. Klaseboer, V. V. Wong, R. Dumke and C.-D. Ohl, *Proc. Natl. Acad. Sci. U. S. A.*, 2011, **108**, 5996–5998.
- 249 D. Fernandez Rivas, M. Ashokkumar, T. Leong, K. Yasui, T. Tuziuti, S. Kentish, D. Lohse and H. J. G. E. Gardeniers, *Ultrason. Sonochem.*, 2012, **19**, 1252–1259.
- 250 K. Thangavadeivel, M. Konagaya, K. Okitsu and M. Ashokkumar, *J. Environ. Chem. Eng.*, 2014, **2**, 1841–1845.
- 251 A. Hommes, A. J. ter Horst, M. Koeslag, H. J. Heeres and J. Yue, *Chem. Eng. J.*, 2020, **399**, 125750.
- 252 Z. Peng, G. Wang, B. Moghtaderi and E. Doroodchi, *Chem. Eng. Sci.*, 2022, **247**, 117040.
- 253 J. Zong and J. Yue, *Front. Chem. Eng.*, 2022, **3**, 788241.
- 254 J. Zong and J. Yue, *Ind. Eng. Chem. Res.*, 2022, **61**, 6269–6291.
- 255 R. Singuru, Q. T. Trinh, B. Banerjee, B. Govinda Rao, L. Bai, A. Bhaumik, B. M. Reddy, H. Hirao and J. Mondal, *ACS Omega*, 2016, **1**, 1121–1138.
- 256 J. Mondal, Q. T. Trinh, A. Jana, W. K. H. Ng, P. Borah, H. Hirao and Y. Zhao, *ACS Appl. Mater. Interfaces*, 2016, **8**, 15307–15319.

- 257 B. Boro, R. Paul, H. L. Tan, Q. T. Trinh, J. Rabeah, C.-C. Chang, C.-W. Pao, W. Liu, N.-T. Nguyen, B. K. Mai and J. Mondal, *ACS Appl. Mater. Interfaces*, 2023, **15**, 21027–21039.
- 258 T. N. A. Mai, M. S. Hossain, N. M. Nguyen, Y. Chen, C. Chen, X. Xu, Q. T. Trinh, T. Dinh and T. T. Tran, *Adv. Funct. Mater.*, 2025, 2500714, DOI: [10.1002/adfm.202500714](https://doi.org/10.1002/adfm.202500714).
- 259 A. F. Fischer, T. Bahry, Z. Xie, K. Qian, R. Li, J. Kwan, F. Jerome, S. Valange, W. Liu, P. N. Amaniampong and T. S. Choksi, *ChemSusChem*, 2024, **17**, e202400838.
- 260 L. Rekhi, Q. T. Trinh, A. M. Prabhu and T. S. Choksi, *ACS Catal.*, 2024, **14**, 13839–13859.
- 261 Q. T. Trinh, K. Bhola, P. N. Amaniampong, F. Jérôme and S. H. Mushrif, *J. Phys. Chem. C*, 2018, **122**, 22397–22406.
- 262 Q. T. Trinh, A. Banerjee, Y. Yang and S. H. Mushrif, *J. Phys. Chem. C*, 2017, **121**, 1099–1112.
- 263 Q. T. Trinh, A. V. Nguyen, D. C. Huynh, T. H. Pham and S. H. Mushrif, *Catal. Sci. Technol.*, 2016, **6**, 5871–5883.
- 264 Q. T. Trinh, K. F. Tan, A. Borgna and M. Saeys, *J. Phys. Chem. C*, 2013, **117**, 1684–1691.
- 265 K. Bhola, Q. T. Trinh, D. Liu, Y. Liu and S. H. Mushrif, *Catal. Sci. Technol.*, 2023, **13**, 6764–6779.
- 266 G. Liu, Q. T. Trinh, H. Wang, S. Wu, J. M. Arce-Ramos, M. B. Sullivan, M. Kraft, J. W. Ager, J. Zhang and R. Xu, *Small*, 2023, **19**, 2301379.
- 267 R. Paul, S. C. Shit, T. Fovanna, D. Ferri, B. Srinivasa Rao, G. T. K. K. Gunasooriya, D. Q. Dao, Q. V. Le, I. Shown, M. P. Sherburne, Q. T. Trinh and J. Mondal, *ACS Appl. Mater. Interfaces*, 2020, **12**, 50550–50565.
- 268 C. Sarkar, S. Pendem, A. Shrotri, D. Q. Dao, P. Pham Thi Mai, T. Nguyen Ngoc, D. R. Chandaka, T. V. Rao, Q. T. Trinh, M. P. Sherburne and J. Mondal, *ACS Appl. Mater. Interfaces*, 2019, **11**, 11722–11735.
- 269 A. F. Fischer, T. Bahry, Z. Xie, R. Batista, da S. Junior, K. Qian, R. Li, J. Kwan, F. Jerome, S. Valange, W. Liu, P. N. Amaniampong and T. S. Choksi, *ChemSusChem*, 2025, e202500097, DOI: [10.1002/cssc.202500097](https://doi.org/10.1002/cssc.202500097).
- 270 P. T. Anastas and J. C. Warner, *Green Chemistry: Theory and Practice*, Oxford University Press, Oxford, 1998.
- 271 P. Cintas and J.-L. Luche, *Green Chem.*, 1999, **1**, 115–125.
- 272 G. Cravotto and P. Cintas, *Chem. Sci.*, 2012, **3**, 295–307.
- 273 M. Draye, J. Estager and N. Kardos, in *Activation Methods: Sonochemistry and High Pressure*, ed. J.-P. Goddard, M. Malacria and C. Ollivier, Wiley ISTE, 2019, pp. 1–93.
- 274 M. Draye and N. Kardos, *Top. Curr. Chem.*, 2016, **374**, 74.
- 275 M. Draye, G. Chatel and R. Duwald, *Pharmaceuticals*, 2020, **13**, 23.
- 276 I. V. Machado, J. R. N. dos Santos, M. A. P. Januario and A. G. Corrêa, *Ultrason. Sonochem.*, 2021, **78**, 105704.
- 277 A. Režek Jambrak, A. G. Da Cruz and J. Chen, *Ultrason. Sonochem.*, 2024, **106**, 106880.
- 278 S. C. Ameta, R. Ameta and G. Ameta, *Sonochemistry: An Emerging Green Technology*, Apple Academic Press, New York, 2018.
- 279 D. Fernandez Rivas, P. Cintas, J. Glassey and D. C. Boffito, *Ultrason. Sonochem.*, 2024, **103**, 106795.
- 280 P. T. Anastas and J. B. Zimmerman, *Environ. Sci. Technol.*, 2003, **37**, 94A–101A.
- 281 T. J. Mason, *Ultrason. Sonochem.*, 2007, **14**, 476–483.
- 282 G. Chatel, *Sonochemistry: New Opportunities for Green Chemistry*, World Scientific Publishing, Singapore, 2017.
- 283 V. Sivakumar and P. G. Rao, *Trans. Indian Natl. Acad. Eng.*, 2024, **9**, 1–24.
- 284 G. Chatel, *Ultrason. Sonochem.*, 2018, **40**, 117–122.
- 285 S. L. Fegade and J. P. Tremblay, *Ultrason. Sonochem.*, 2017, **37**, 686–687.
- 286 P. Cintas, *Ultrason. Sonochem.*, 2016, **28**, 257–258.